

Deliverable 3.1: Dynamic building stock analysis



MODERATE

Marketable Open Data Solution for Optimized Building-related Energy Services



Table of Contents

- Table of Contents 1
- List of Figures 3
- List of Tables 4
- Executive Summary 6
- 1. Introduction 8
 - 1.1. Building Sector Environmental Impact 8
 - 1.2. European Directives 8
 - 1.3. Building Stock Data 9
 - 1.4. Case Studies 12
- 2. Case Study I: EPCs Classification form Satellite Images 14
 - 2.1. Methodology 15
 - 2.1.1. Data Curation 15
 - 2.1.2. Classification Model 17
 - 2.2. Results 19
 - 2.3. Discussion 22
 - 2.3.1. Quantify Economical Feasibility 23
- 3. Case Study II: Photovoltaic Data Extraction from Aerial Imagery 24
 - 3.1. Methodology 26
 - 3.1.1. Detection of Rooftop Mounted Photovoltaic Installations from Aerial Imagery 26
 - 3.1.2. Capacity Estimation of Detected Photovoltaic Installations 28
 - 3.1.3. Context 28
 - 3.2. Application of the Methodology 30
 - 3.2.1. Data 30
 - 3.2.2. Manual Annotation of Photovoltaic Installations 30
 - 3.2.3. Image Processing 31
 - 3.2.4. Detection of Rooftop Mounted Photovoltaic Installations from Aerial Imagery 32
 - 3.3. Results 33
 - 3.3.1. Detection of Rooftop Mounted Photovoltaic Installations from Aerial Imagery 33
 - 3.3.2. Capacity Estimation of Detected Photovoltaic Installations 35
 - 3.4. Discussion 36
 - 3.4.1. Quantify Economical Feasibility 37
- 4. Case Study III: Analysis Photovoltaic Distribution in Relation to Urban Morphology from Aerial Imagery 38
 - 4.1. Methodology 38



4.2.	Results	40
4.3.	Discussion	45
4.3.1.	Quantify Economical Feasibility	45
5.	Conclusions	46
	References	48



List of Figures

Figure 1. Remote sensing approach from data to knowledge.....	11
Figure 2. Energy Performance Certificate classes.....	14
Figure 3. Results of the geocoding building addresses.....	16
Figure 4. Example of building footprints from pen Street Maps.....	17
Figure 5. Available data after each step of the data curation process: Step 1 - filter EPCs data from CENED+2 database; Step 2 - geocoding building addresses; Step 3 - data cleaning; Step 4 - download satellite images; Step 5 - obtain building footprints and temperature data; Step 6 - combine data...	19
Figure 6. Frequency of buildings Energy Performance Certificates (n = 26 192).....	20
Figure 7. Model confusion matrix.....	22
Figure 8. Steps for the application of machine learning techniques on imagery..	27
Figure 9. Photovoltaic Power Potential in Spain.....	29
Figure 10. Manual annotation of PV installations at the municipal stadium.....	30
Figure 11. Manual annotation of PV installations on the roof of an industrial building.....	31
Figure 12. Seamlines detected within Crevillent.....	32
Figure 13. Examples of results of logistic regression in detecting photovoltaic installations..	34
Figure 14. Examples of results of logistic regression in detecting photovoltaic installations..	34
Figure 15. Examples of results of logistic regression in detecting photovoltaic installations..	35
Figure 16. Example of detection of a photovoltaic installations.....	36
Figure 17. Examples of results of detection of buildings from aerial imagery using Mapflow..	39
Figure 18. Industrial polygons of Crevillent.....	39
Figure 19. Number of buildings with PV installation per zone. Scale 1:40000.....	41
Figure 20. Area of PV installation per zone. Scale 1:40000.....	42
Figure 21. Average Area Roofs with PV installations per zone. Scale 1:40000.....	43
Figure 22. Average height of buildings with PV installations per zone. Scale 1:40'000..	44



List of Tables

Table 1. Model performance comparison.	20
Table 2. Selected model performance.....	21
Table 3. Single Energy Performance Certificates classes metrics.....	21



PROJECT DURATION: 1 June 2022 – 31 May 2026

WP: 3 DELIVERABLE: D3.1 Dynamic building stock analysis

LEAD BENEFICIARY: EURAC

SUBMISSION DATE: 31st of May 2023

DISSEMINATION LEVEL: Public

DUE DATE: final version M12

REVISION HISTORY:

DATE	VERSION	AUTHOR/CONTRIBUTOR	REVISION BY	COMMENTS
31/05/2023	1	Fabio Giussani, Claudio Zandonella Callegher, Eric Wilczynski, and Simon Pezzutto (EURAC)	Yixiao Ma (VITO), Philipp Mascherbauer (TUW)	/

Disclaimer: The information in this document is provided as is and no guarantee or warranty is given that the information is fit for any particular purpose. The user thereof uses the information at its sole risk and liability. The document reflects only the author’s views and the Agency is not responsible for any use that may be made of the information contained therein.

Acknowledgements:



This project has received funding from the European Union’s Horizon Europe research and innovation programme under grant agreement No 101069834. Views and opinions expressed are however those of the author(s) only and do not necessarily reflect those of the European Union or CINEA. Neither the European Union nor the granting authority can be held responsible for them.

© Copyright MODERATE Consortium This document may not be copied, reproduced, or modified in whole or in part for any purpose without written permission from MODERATE Consortium. In addition to such written permission to copy, reproduce, or modify this document in whole or part, an acknowledgement of the authors of the document and all applicable portions of the copyright notice must be clearly referenced. All rights reserved.



Executive Summary

The building sector plays a crucial role in the achievement of the European climate neutrality goal by 2050. In fact, the building sector accounts for 36% of global energy use and 37% of energy-related greenhouse gas emissions. Therefore, effective policy initiatives and directives aimed at reducing greenhouse gas emissions, promoting sustainable energy use, and improving energy efficiency in the building sector are fundamental.

However, to inform policy makers decisions, accurate and reliable data on the building stock are required. Precise and accurate information are needed by policymakers to monitor the current state of the building stock and obtain useful insights regarding its future development. In this way, they can develop tailored measures to obtain the best improvements.

There are two main approaches for the collection of data regarding the building stock: the top-down approach (i.e., using aggregated data at the national or regional level, based on statistical models and assumptions) and the bottom-up approach (i.e., collecting data on individual buildings). Data obtained through top-down approaches are useful to analyse building stock dynamics and broad patterns on a larger scale, however, they lack the required granularity for implementing specialized strategies is significantly hindered. On the contrary, bottom-up approach provide very detailed information but is extremely time-consuming and expensive.

Remote sensing can become an ideal data source to overcome these limitations. Remote sensing can provide reliable and detailed information in an automated and economically feasible way. Although, application of remote sensing in the collection of data regarding the building stock are scarce in the scientific literature, results are promising.

In this Deliverable, we presented three case studies based on remote sensing data for the analysis of different aspects of the building stock. Accuracy and reliability of the proposed approaches were evaluated as well as their economic feasibility.

- In Chapter 2, we propose a methodology for automatically classifying building energy performance certificates (EPCs) based on the analysis of satellite images. When compared to the baseline score obtained at chance level (i.e., 14% accounting for the presence of 7 different EPCs classes), the obtained results provide a 5% improvement. Although these improvements are moderate, current results provide a first indication of the potential for using satellite images on the classification of EPCs. This approach is still at its initial phases and further improvements are required to overcome the current limitations. However, this approach has the potential to provide an efficient and cost-effective method for assessing the energy performance of buildings on a large scale.
- In Chapter 3, we present an approach based on aerial images to detect installed photovoltaic panels and estimate the installed photovoltaic capacity on rooftops in urban areas. The model is used to estimate the photovoltaic (PV) capacity installed in the town of Crevillent, Spain. Following this approach, large scale areas can be evaluated, and results could provide valuable information for urban planners and policymakers in promoting renewable energy adoption. The used method was chosen for its low training requirements compared to more complex algorithms. The validation method of Intersection over Union achieved a score of 0.67 based on a list of addresses with PV installations serving as ground truth data. The result does not provide an accuracy as high as other algorithms, but the low amount of training required justifies the choice of the method.



- In Chapter 4, we focus on an analysis of the distribution of PV installations in industrial and residential areas. First, footprints of buildings are detected by a machine learning algorithm using a GIS plugin. Then, the identified buildings are integrated with the information about existing PV installations. Finally, the vectorial data is merged with a normalized Digital Surface Model and with bottom-up information on the land use. This serves as a basis for the analysis of different variables: land use of the area, either residential or industrial; number of buildings with PV installations; total area of PV installations; height of buildings with PV installations and square footage of roofs hosting PV installations. The results obtained in this case study reflect the relationship between urban morphology, in particular urban density, and photovoltaic installations that emerges from literature on the topic. The larger amount of photovoltaic surface is present in industrial areas connotated by lower building density.

Overall, the results obtained from the three case studies provide a clear hint on the potential of using remote sensing for the collection of data regarding the European building stock. Remote sensing can provide reliable and detailed information in an automated and economically feasible way. However, remote sensing is still in its initial stages of development and further research is required to fully exploit its potential.



1. Introduction

The announcement of the Green Deal [1] by the European Commission in 2019 signalled the EU's commitment to achieving climate neutrality by 2050. The Green Deal encompasses a wide range of policy initiatives aimed at reducing greenhouse gas (GHG) emissions, promoting sustainable energy use, and improving energy efficiency across various sectors of the economy. One critical sector that requires significant transformations to achieve the Green Deal's goals is the building sector.

1.1. Building Sector Environmental Impact

The building sector is responsible for a considerable proportion of GHG emissions and energy consumption, making it a key area for action. According to the United Nations Environment Programme [2], the building sector is a major contributor to both energy consumption and GHG emissions, accounting for 36% of global energy use and 37% of energy-related GHG emissions.

GHG emissions and energy consumption in the building sector are determined not only by the operational requirements of already existing buildings such as space heating, space cooling, lighting, and ventilation, but also by the carbon footprint of the materials and the emissions produced in the construction of new buildings. In fact, a large share of GHG emissions associated with the building sector is caused by the production of building materials and building operation [2], [3].

The construction industry is the biggest global user of raw materials accounting for almost 60% of all materials used by humanity [4]. The extraction, transportation, manufacturing, and assembly of building materials require significant amounts of energy, contributing to a large part of the GHG emissions associated with the building sector [5]–[7]. According to recent reports, around 11% of the GHG emissions associated with the building sector are attributed to the manufacturing of building materials and products, while around 28% are attributed to the operation of buildings [2], [3].

Moreover, the building sector generates large amounts of construction and demolition waste (CDW), which pose significant environmental challenges. The CDW includes materials such as concrete, wood, and steel, which contribute to the depletion of natural resources and the emission of GHGs [8]. In the European Union (EU), CDW constitutes about 25-30% of the total generated solid waste [9].

Overall, the building sector plays a vital role in achieving climate neutrality. Therefore, efforts to enhance sustainability in the building sector must address all its elements, from the improvement in energy efficiency of already existing buildings, to the reduction of material consumption and proper management of CDW.

1.2. European Directives

The Green Deal recognizes the need for urgent action to address the environmental impact of building sector and defines a comprehensive set of policy initiatives aimed at enhancing the transition towards a climate-neutral building sector.

The Renovation Wave strategy is a policy initiative established by the European Commission that seeks to improve building energy efficiency and promote the use of renewable energy sources in the building sector [10]. The strategy intends to double the rate of renovation in the EU by 2030, which is expected to create new jobs, stimulate economic growth, and reduce energy consumption and greenhouse gas emissions. The Renovation Wave aims to make buildings in the EU more energy-efficient, comfortable,



and healthy, while also reducing energy poverty, by supporting the renovation of public and private buildings, including residential, commercial, and public buildings.

Similarly, the Energy Performance of Buildings Directive (EPBD) is a policy initiative that aims to improve the energy efficiency of buildings in the EU [11]. The EPBD defines minimum energy performance standards for new and existing buildings, encourages the use of smart technologies, and aims to make buildings more sustainable and climate friendly. The directive requires EU countries to develop long-term renovation strategies for the building stock, which include energy-efficient measures, the use of renewable energy sources, and the reduction of greenhouse gas emissions.

Moreover, the New European Bauhaus is a policy initiative established by the European Commission that aims to create a framework for designing and building sustainable, inclusive, and aesthetically pleasing environments in the EU [12]. The New European Bauhaus aims to integrate design, sustainability, and innovation to create buildings that are not only functional but also attractive and environmentally friendly. The initiative seeks to promote social and economic development by creating a new generation of buildings that are energy-efficient, accessible, and inclusive, and that contribute to the well-being of people and the environment.

Finally, the EU has put forth a comprehensive plan to promote a sustainable built environment through the use of Circular Economy (CE) principles [13]. The EU Strategy for a Sustainable Built Environment aims to incorporate CE principles throughout the lifecycle of buildings. This includes strategies for urban mining and building material reuse, which recognize waste as a valuable resource. The strategy also promotes sustainable construction practices to reduce waste production and increase the use of recycled materials. To enhance the value of building materials and prolong their durability, the H2020 Building As Materials Banks (BAMB) project has been funded [14]. The project is committed to developing innovative approaches to material recovery and reuse in the building sector.

Overall, these policy initiatives aim to reduce the energy consumption of the building sector in the EU by setting new energy efficiency standards and promoting the reconstruction and renovation of the existing building stock. The initiatives seek to make buildings more sustainable, comfortable, and healthy, while also reducing energy poverty and greenhouse gas emissions. Moreover, the implementation of CE principles in the building sector can lead to a more sustainable and resource-efficient industry. Through the recycling and reuse of building materials and the promotion of sustainable construction practices that minimize waste and limit resource consumption, the environmental impact of the construction sector can be significantly reduced. All these policy initiatives are essential in achieving the EU's climate goals and promoting a more sustainable and resilient future.

1.3. Building Stock Data

To enhance the transition towards a climate-neutral building sector, detailed information regarding the building stock is required. Collecting data on the EU building stock is crucial for several reasons.

Firstly, precise and accurate information is needed by policymakers to monitor the current state of the building stock and obtain useful insights regarding its future development. This allows them to identify areas of inefficiency and develop effective policies to address them. This can include measures to reduce energy consumption, promote renewable energy sources, and improve the sustainability of the built environment.

Secondly, data collection can help to monitor the effectiveness of existing policies and evaluate the impact of new initiatives. By measuring changes in energy consumption, emissions, and other key



indicators, policymakers can determine whether their policies are achieving their intended goals and make adjustments as needed.

Thirdly, data on the building stock can be used to inform decision-making by building owners, investors, and other stakeholders. By providing information on the energy performance and sustainability of buildings, data can help these stakeholders make informed decisions about building design, construction, and operation.

Finally, data on the building stock can support research and innovation in the building sector. By providing a comprehensive picture of the state of the built environment, data can help researchers identify new opportunities for improving energy efficiency, reducing emissions, and promoting sustainability.

There are two main approaches used for collection of data regarding the building stock:

- **Top-Down Approach.** Top-down data collection refers to an approach that uses aggregated data at the national or regional level, based on statistical models and assumptions. This approach relies on data such as energy consumption and greenhouse gas emissions at the national level and then estimates the energy performance of buildings based on these macro-level data. Top-down data collection is useful for providing a general overview of the building stock considering its general characteristics and trends over time at a national level. However, this approach has limitations, as it relies on assumptions and provides only approximations that may not reflect the actual characteristics of buildings in a specific individual region.
- **Bottom-Up Approach.** Bottom-up data collection refers to an approach that collects data on individual buildings, typically through surveys and on-site measurements. This approach involves collecting detailed data on the building's physical characteristics, energy systems, and occupant behaviour to estimate, for example, its energy performance. Bottom-up data collection provides more accurate and detailed information regarding specific individual buildings, allowing for targeted dedicated measures. However, this approach is more time-consuming and expensive than top-down data collection.

Data collected using a top-down approaches are normally used to study building stock dynamics and general patterns at a larger scale. These results are useful to inform policymakers and monitor environmental performances at a national level. However, top-down data collection provides results in a highly aggregated form that may not be representative of the actual characteristics of buildings in a specific region. This aspect severely limits the utility of top-down collected data for the implementation of dedicated strategies.

Informing and applying dedicated strategies requires accurate and detailed data regarding the specific individual buildings that can only be obtained by a bottom-up approach. Only by collecting data with high level of granularity and spatial definition, ad hoc solutions can be evaluated and implemented. However, bottom-up approaches are extremely time-consuming and expensive. In this regard, remote sensing is an excellent complement approach that can help in overcoming these issues.

Remote sensing is the process of acquiring information about an object, area, or phenomenon without physically being in contact with it. It involves the use of various technologies such as aerial photography, radar, LiDAR, and satellite imagery to gather data from a distance. Collected data using remote sensing can be then used to analyse and understand the characteristics, properties, and behaviour of objects and environments on the Earth's surface, as well as monitor and detect changes over time. The quality, detail, and accuracy of the data provided by remote sensing, coupled with its cost-effective method of data collection, make it a popular choice for many applications. Among

others, remote sensing has been applied in fields such as environmental monitoring, agriculture, forestry, and natural resource management.

In this respect, remote sensing can be an effective tool for collecting data also regarding the building sector. This is because remote sensing technologies, such as satellite imagery and aerial photography, can provide detailed information about the physical characteristics of buildings, such as their size, shape, and location. These data can then be used to model and provide valuable insights regarding other characteristics of buildings, such as their energy performance, as well as their structural and environmental characteristics. Information obtained from remote sensing are excellent complement to statistics and can be applied in both top-down and bottom-up approaches (please see Figure 1).



Figure 1. Remote sensing approach from data to knowledge.

In the scientific literature, there is an increasing interest in the application of remote sensing for the collection of data related to the building stock. Different studies proposed the use of remote sensing data to evaluate various aspects of the building stock. Wurm et al. [15] presented a workflow for modelling the building stock using deep learning techniques, which involves the use of aerial images to estimate the space heating demand of residential buildings based on their construction type and period at a city scale. Furthermore, the investigation assessed multiple renovation strategies targeting various building types and timeframes in order to pinpoint areas of inefficiency and prioritize intervention.

Considering the quantification of materials, Haberl et al. [16] presented an approach for broad-scale material stock mapping based on freely available high-resolution earth-observing imagery and OpenStreetMap data. While material stock maps derived from cadastral data are more accurate for establishing resource cadasters in individual cities, this method can provide a compromise between coarse material stock estimates from night-time lights and detailed cadastral-based studies. The method is based on freely available data, can be extended over national areas, and can be replicated over any time span for which satellite and crowd-sourcing data, training data for assessing the height of buildings, and robust material intensity factors are available. This novel method can provide an improved high-resolution mapping to investigate urbanization, urban form, and infrastructure developments and inform infrastructure vulnerability studies.

Bao et al. [17] proposed an end-to-end deep-learning model for high-resolution quantification of building stock using multi-source remote sensing data, including optical remote sensing and spatiotemporal features from night time light data. Their approach allows for the reliable estimation of building stock and provides insight into the spatial concentration of materials, urban mining potential, and sustainable urban development. The study demonstrated the significant potential of

remote sensing imagery and deep learning for stock estimation and suggested that large-scale, long-term building-stock investigations could benefit from this approach's predictability and data availability.

Similarly, Arbabi et al. [18] develop a framework that can automate the characterization of urban stock at a building component level. To achieve this, the researchers proposed a scalable approach that combines mobile sensing and computer vision to capture urban stocks as 3D surface maps. This framework can enable the identification and semantic classification of stock objects, components, and materials, leading to a higher resolution of details. By using this approach, the researchers aim to improve the understanding of the urban stock and enable better decision-making towards sustainable urban development.

Rajaratnam et al. [19] investigated the research maturity of GIS, remote sensing, spatial analysis, and complementary methods adopted in building stocks mining and CE studies using a systematic literature review. Their results highlighted five research trends of GIS and remote sensing in BS mining and CE studies. These are (i) the development of locational building stock data, (ii) enhancement of the accuracy of building stock data, (iii) the introduction of automatic technique to reduce the time of building stock estimation and locating the building stock, (iv) analysing the spatial and temporal patterns of building stock using both backcasting and forecasting approaches, and finally (v) the application and policy-orientated research.

Overall, all these studies highlighted the potential and benefits of implementing remote sensing solution for the collection of data related to the building stock. Despite these initial results, however, the application of remote sensing for the collection of data related to the building stock is still at its initial stages and further research is required to fully develop its capabilities.

1.4. Case Studies

In the following chapters, we present three case studies exploring the application of remote sensing for the collection of data related to the building stock in new contexts. In particular:

- In Chapter 2, we propose a method for automatically classifying building energy performance certificates based on the analysis of satellite images. This method utilises machine learning algorithms to extract features from satellite images and link them to building energy performance certificates. This approach has the potential to provide an efficient and cost-effective method for assessing the energy performance of buildings on a large scale, which could inform policies and interventions for energy efficiency in the built environment.
- In Chapter 3, we present an approach based on aerial images to detect installed photovoltaic panels and estimate the installed photovoltaic capacity on rooftops in urban areas. This approach uses high-resolution aerial images combined with object-based image analysis and machine learning techniques to identify and classify photovoltaic panels on rooftops. Following this approach, large scale area can be evaluated, and results could provide valuable information for urban planners and policymakers in promoting renewable energy adoption.
- In Chapter 4, we investigate the relationship between urban residential and industrial areas with respect to presence of PV installations. First, footprints of buildings are detected by machine using a GIS plugin and integrated with the previously detected PV installations. Then, the vectorial data is merged with a normalized Digital Surface Model (DSM) and with bottom-up information on the land use. This allows for the analysis of different variables: land use of the area, either residential or industrial; number of buildings with PV installations; total area



of PV installations; height of buildings with PV installations and square footage of roofs hosting PV installations.



2. Case Study I: EPCs Classification form Satellite Images

Energy Performance Certificates (EPCs) are a rating schema summarising energy efficiency of buildings in a standardized way [20]. EPCs consider factors such as insulation, space heating, space cooling, lighting, and ventilation systems and assign an energy rating for the building, ranging from A (very energy efficient) to G (very inefficient, see Figure 2). In addition, EPCs include recommendations for how to improve the building's energy performance.



Figure 2. Energy Performance Certificate classes.

EPCs are required by law in all EU countries and play a central role in the Energy Performance of Buildings Directive [11]. In fact, EPCs are used to set energy performance standards and compare the energy efficiency of different buildings. Data regarding the EPCs are useful for monitoring the current state of energy efficiency of the building stock. Policy makers can use this information to design and implement policies and programs aimed at improving energy efficiency and reducing greenhouse gas emissions in the building sector. For example, they can use data related to EPCs to identify areas where energy efficiency improvements are most needed and target incentives or regulations to encourage building owners to make these improvements. In addition, they can also use EPC data to track the effectiveness of existing policies and programs aimed at improving energy efficiency in buildings.

Data regarding the EPCs, however, are not easily available. The main issue is the lack of a centralized database. In fact, in many countries, there is not a single database that collects and stores EPC data for all buildings. Instead, in most cases, EPC data is spread across multiple databases that may be neither publicly available nor geographically complete. Therefore, new solutions are required to efficiently collect data on buildings' EPCs and allow large-scale analyses informing policy makers decisions.

In the literature, several studies investigated the impact and role of EPCs in the development of the European building stock. Charalambides et al. [21] confirmed how EPCs did play a role both in renovation decisions and the promotion of investment for deep energy renovation of buildings. Furthermore, they highlighted the potential benefits and effectiveness of using retrofitting online tools providing suggestions on increasing the deep energy renovation market in Europe. Similarly, Li et al. [22] pointed out how the introduction of EPCs favour the creation of a demand-driven market

for energy-effective buildings. Finally, Pasichnyi et al. [23] reviewed existing applications of EPC data showing how, apart from ‘traditional’ areas of EPC data applications (mapping building energy performance or analysis; effect of EPC on real estate market), novel areas of application are emerging (building energy retrofiting, energy planning, investment analysis, market popularity of retrofiting solutions).

Although most studies pointed out the issues related to the limited availability of data regarding EPCs, only Mayer et al. [24] proposed an automated method for estimating building energy efficiency using remote sensing data. Starting from street view imagery, aerial imagery, and land surface temperature data, they classified buildings EPCs using end-to-end deep learning models. Their work shows the potential and complementary nature of remotely sensed data in predicting energy efficiency. However, they only classified buildings into two categories energy efficient (EU rating A–D) or inefficient (EU rating E–G).

In the present case study, we further explore the use of remote sensing by proposing an approach for the classification of buildings EPCs based on satellite images. In doing that, we consider separately all the 7 buildings EPCs classes (from A to G).

2.1. Methodology

Public databases that offer standardized and widely available energy efficiency ratings at the building level remain scarce. The Italian region Lombardy, however, freely provides a detailed dataset covering all the buildings EPCs in its territory. Therefore, we considered Lombardy as an ideal choice for the present case study.

2.1.1. Data Curation

In the present case study, data were collected from the following data sources:

- **Database CENED+2 - Certificazione ENergetica degli Edifici** [25]. Data regarding the buildings EPCs in the Italian region Lombardy. This dataset includes around 1.39 million data entries regarding dwellings and buildings EPCs ranging from rom A (most efficient) to G (least efficient).
- **Copernicus SENTINEL-2 Satellite Images** [26]. SENTINEL-2 satellite is part of the Copernicus Programme operated by the European Space Agency (ESA). It provides Earth observation data for environmental monitoring and security purposes with high-resolution multispectral imagery of the Earth's surface. Obtained images have a spatial resolution up to 10 meters and data are provided for 13 different spectral bands, ranging from visible and near-infrared to shortwave infrared, at different spatial resolutions.
- **Open Street Maps** [27]. OpenStreetMap is a collaborative, open-source platform for mapping and geospatial data, where contributors can add and edit information such as building footprint polygons, roads, and other features.
- **Copernicus Climate Data Store ERA5** [28]. ERA5 (fifth generation of atmospheric reanalysis of the global climate) is a dataset produced by the European Centre for Medium-Range Weather Forecasts (ECMWF) that provides hourly estimates of a range of atmospheric, oceanic and land surface variables. In particular, we considered the temperature of air at 2 meters above the surface of land.

Note that all datasets listed above are freely available and released under open licenses. To prepare the data for the analysis, we followed the following steps:

1. Step 1 – Filter EPC Data: Data from CENED+2 Database was downloaded and filter to keep only values referring to whole buildings (i.e., excluding EPCs of single dwellings within a building). Moreover, considering Sentinel images spatial resolution (i.e., 10m), buildings with an area smaller than 100 m² were excluded as they would cover less than 1 pixel. Finally, only buildings with complete information for the address and other building characteristics (e.g., construction year) were considered.
2. Step 2 – Geocoding Building Addresses: Three different providers were used to geocode building addresses: Open Street Map API [29], Bing Maps [30], and Google Maps [31]. Points that were wrongly geolocated outside of their respective municipality were excluded (please see Figure 3).

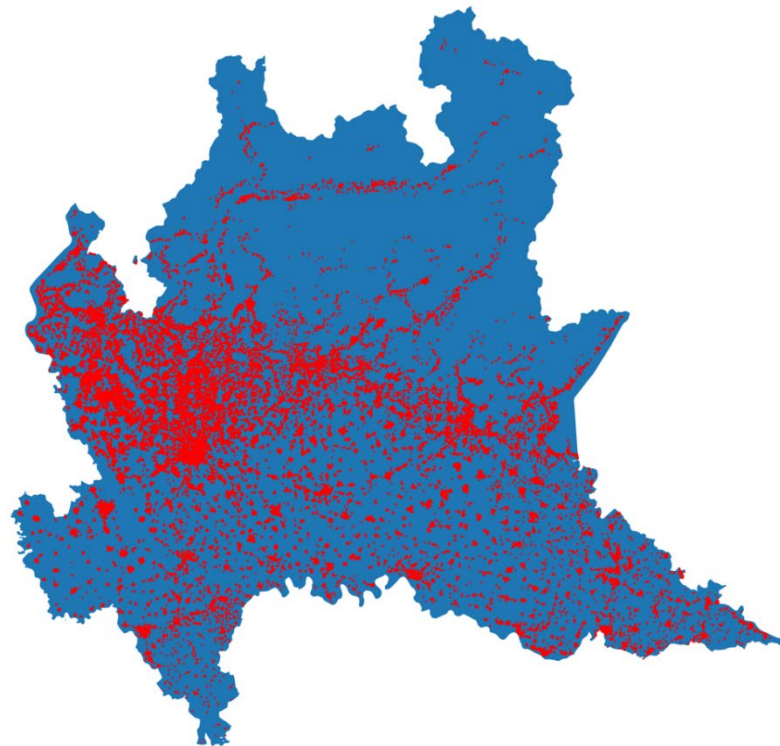


Figure 3. Results of the geocoding building addresses.

3. Step 3 – Data Cleaning: Buildings subject to important rebuilding or buildings subject to energy performance requalification were excluded as they can potentially decrease the correlation between information the variable of interest.
4. Step 4 – Download Satellite Images: Satellite images from Sentinel 2 (Level 2A) covering Lombardy region were downloaded using the openEO Python Client [32]. To minimize the presence of clouds in the images, we inspected all available dates and selected '2022-01-11' (winter season) and '2022-08-14' (summer season) dates as they presented the best meteorological condition (i.e., low percent of clouds). Thus, for each building we obtained two images, one during the winter season and the other summer season.
5. Step 5 – Obtain Building footprints and Temperature Data: Raster data with the building footprints of all Lombardy region was downloaded from Open Street Map API. Geocoded addresses were associated to building footprints by considering the nearest building within a maximum distance of 50 meters (please see Figure 4).
Data regarding the air temperature at 2 meters above the surface of land was downloaded from ERA5 datasets considering '2022-01-11' (winter season) and '2022-08-14' (summer

season) dates. In both cases, we used values registered at 10.00 AM as they represent the closest available values to when satellite images were taken.

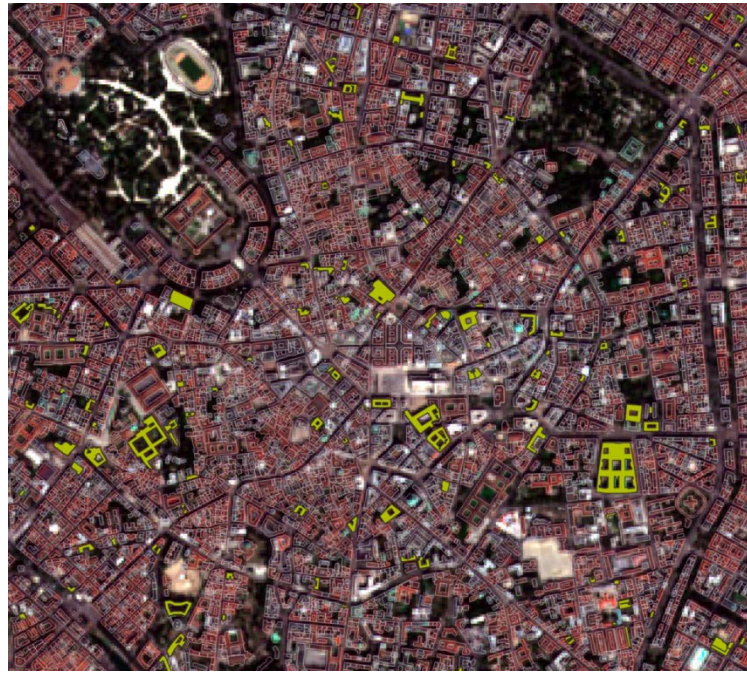


Figure 4. Example of building footprints from pen Street Maps.

6. **Step 6 – Combine Data:** Information collected in previous steps was combined to obtain the data used in the analysis. For each building, we associated the respective winter and summer temperature obtained from ERA5 dataset. Moreover, building footprints were used to crop respective pixels from winter and summer satellite images. For each different band, minimum, mean and maximum values were computed. Obtained data were finally filtered to remove buildings with high levels of clouds or shadows in their pixels.

Summarizing, for each building included in the analysis we obtained its EPC (from A to G), the minimum, maximum, and average band values of the building footprints pixels from the winter and summer satellite images, and the respective winter and summer air temperatures.

2.1.2. Classification Model

To classify buildings EPCs using the information obtained from the satellite images and the temperature values, we compared the performance of different machine learning models:

- Gaussian Naive Bayes Classifier (baseline). The Gaussian Naive Bayes Classifier is often used as a baseline model because it is a simple and computationally efficient algorithm that can provide a reasonable performance for classification tasks. In this way, we can evaluate the effectiveness of more advanced models in improving classification performance. If a more complex model fails to significantly outperform the Naive Bayes Classifier, it suggests that the additional complexity of the model may not be justified and a simpler approach may be sufficient for the task at hand. On the other hand, if a more complex model significantly outperforms the baseline, it indicates that the additional complexity is warranted and may provide valuable insights for improving the classification task.



- Random Forest Classifier. Random Forest is another model commonly used for classification tasks, especially when dealing with high-dimensional data. It is an ensemble learning method that constructs a multitude of decision trees and combines their predictions to produce a final output. Random Forest provides good performance on a wide range of classification problems and is also able to handle non-linear relationships between the features and the target variable capturing complex interactions.
- eXtreme Gradient Boosting (XGBoost) Classifier. XGBoost is a popular machine learning algorithm that is often used for classification and regression tasks. XGBoost is known for its high accuracy and computational efficiency, making it a popular choice for many tasks. It can handle large datasets with a high number of features and can learn complex relationships between the features and the target variable. It also includes several regularization techniques to prevent overfitting and improve generalization performance.

To evaluate the performance of the trained models in the classification of EPCs, we considered different evaluation metrics. Given the imbalanced presences of EPCs classes, we computed precision, recall, and F1 scores for each different class. Precision is the number of true positive predictions divided by the total number of positive predictions (please see Equation (1)). It measures the percentage of positive predictions that are actually correct, or the proportion of correctly identified positive instances out of all instances that were predicted as positive. A high precision indicates that the model is making few false positive errors.

$$Precision = \frac{True\ Positive}{True\ Positive + False\ Positive} \quad (1)$$

Recall is the number of true positive predictions divided by the total number of actual positive instances in the data (please see Equation (2)). It measures the percentage of positive instances that are correctly identified, or the proportion of correctly identified positive instances out of all actual positive instances. A high recall indicates that the model is making few false negative errors.

$$Recall = \frac{True\ Positive}{True\ Positive + False\ Negative} \quad (2)$$

F1 score is the harmonic mean of precision and recall, given by Equation (3). It balances precision and recall and provides a single score that summarizes the performance of the model. A high F1 score indicates that the model is performing well in both precision and recall.

$$F1\ Score = \frac{2}{\frac{1}{Recall} + \frac{1}{Precision}} \quad (3)$$

Subsequently, we computed macro-averaged F1 scores. Macro-averaged F1 score is a way to calculate the F1 score for a multi-class classification problem, where the classes may be imbalanced. In this method, the F1 scores calculated independently for each class are averaged across all classes to get a final score. The macro-averaged F1 score gives equal weight to each class, regardless of the class distribution in the dataset. This means that each class contributes equally to the final score, regardless of the number of samples in the class.

Similarly, we also computed the weighted-average F1 score (i.e., the F1 scores calculated independently for each class are averaged across all classes considering weights inversely proportional

to class frequencies in the data) and the balanced accuracy score (i.e., the average of recall obtained on each class considering weights inversely proportional to class frequencies in the data).

Overall, the considered metrics allowed us to evaluate the performance of the trained models in the classification of EPCs taking into account the imbalanced presences of EPCs classes. Note that all scores motioned above range between 0 and 1 with higher values indicating better performances.

After comparing the performance of the different models, the model providing the best results was selected and presented in the results section. All analyses were conducted using Python 3 [33] and source code is available at: <https://gitlab.inf.unibz.it/URS/moderate>.

2.2. Results

Starting from around 1.39M data available in the CENED+2 Database, more than 70 000 data entries met the requirements indicated in step 1 of the data curation (i.e., EPCs of entire buildings bigger than 100 m² and complete address information). Next, we were able to successfully geocode around 61 000 data, but around 9 000 buildings were removed as they were subject to important rebuilding or energy performance requalification. The reason for excluding these buildings from the analysis is that they represent a distinct subsample with potentially different characteristics compared to other buildings. Therefore, renovated and requalified buildings should be analysed separately. However, due to their limited number, they were excluded from the analysis.

Satellite images for winter and summer season were obtained covering 32 000 buildings, but further 5 000 buildings were removed as no footprint was available from Open Street Map. Final Dataset included in the analysis is based on 26 000 buildings (see Figure 5).

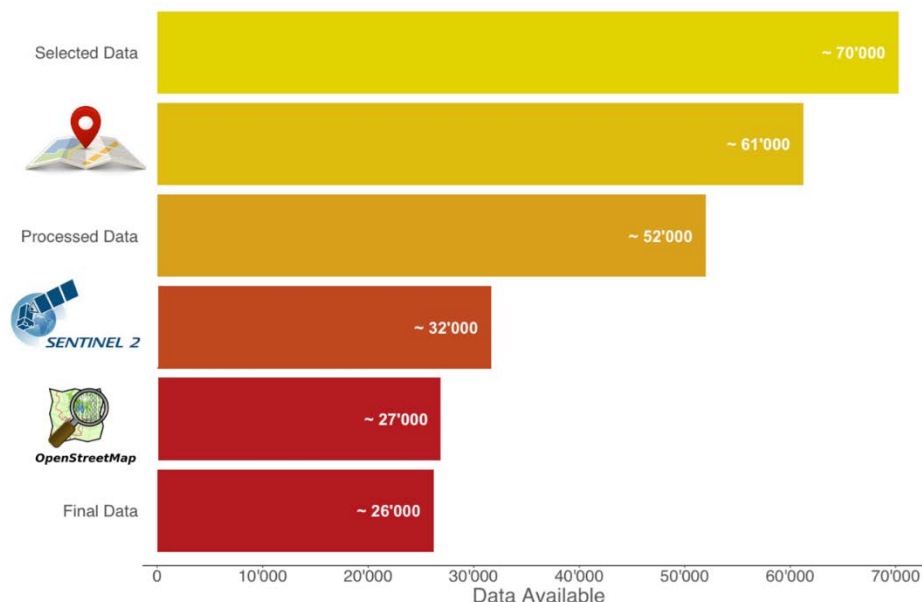


Figure 5. Available data after each step of the data curation process: Step 1 - filter EPCs data from CENED+2 database; Step 2 - geocoding building addresses; Step 3 - data cleaning; Step 4 - download satellite images; Step 5 - obtain building footprints and temperature data; Step 6 - combine data.

In Figure 6, frequencies of the EPCs classes are presented. Most buildings include in the analysis are energy inefficient, with more than one third of buildings belonging to class G. On the contrary, energy efficient buildings (i.e., class A-D) represent only around 27% of the data. Considering these values, it

is important to take into account the high imbalance between EPCs classes when fitting and evaluating the models.

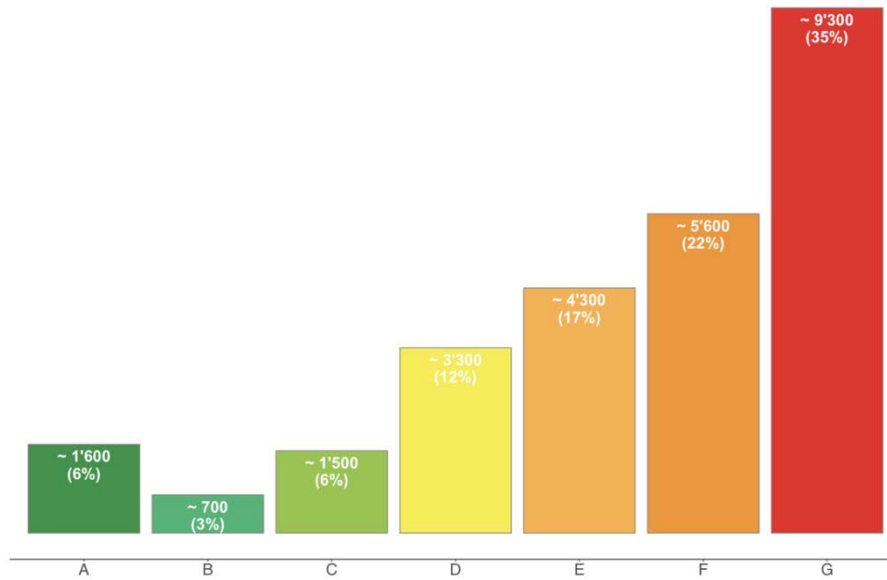


Figure 6. Frequency of buildings Energy Performance Certificates (n = 26 192).

Before training the models, we divided our data into training data (80% of observations) and test data (20% of observations) stratifying by the frequency of EPCs different classes. Subsequently, we normalized the data according to the training values using a min-max scaler.

Balanced accuracy score, macro-average F1 score, and weighted-average F1 score, for the trained models are presented in Table 1. Note that in the Table, also the scores we would obtain at chance level are reported. Values higher than those obtained at chance level represent an improvement in the classification of EPCs.

Table 1. Model performance comparison.

Models	Balanced Accuracy	F1 score	
		Macro-Average	Weighted-Average
Chance level	.142	.125	.088
Gaussian Naive Bayes Classifier (baseline)	0.183	0.165	0.142
Random Forest Classifier	0.172	0.146	0.103
XGBoost Classifier	0.177	0.176	0.147

Considering the Gaussian Naive Bayes Classifier as a baseline, we can observe an improvement in comparison to the chance level. No additional improvements in the classification performance were



achieved by using the Random Forest Classifier. On the contrary, by using the XGBoost Classifier, we were able to obtain an additional small improvement in the classification of EPCs.

By further tuning of the XGBoost hyperparameter (e.g., learning rate, tree depth, and regularization parameters), we obtained a further improvement of the model prediction capabilities. In Table 2, the scores of the final model are reported.

Table 2. Selected model performance.

Models	Balanced Accuracy	F1 score	
		Macro-Average	Weighted-Average
XGBoost Classifier (selected)	0.196	0.189	0.184

To better evaluate the performance of the model, we consider separately the scores for each EPCs class. In Table 3, precision, recall, and F1 Score for each different EPCs class are presented. Moreover, the resulting confusion matrix is provided in Figure 7. A confusion matrix summarizes the performance of a classification model by comparing the predicted class labels to the actual true class labels. It consists of a square grid, with rows representing the true class labels and columns representing the predicted class labels. Cells along the diagonal indicate the number of observations correctly classified (predicted class is equal to the true class), whereas off-diagonal cells represent the number of false positives (observations wrongly assigned to a given class) and false negatives (fail to assignee an observation to its correct class). In the ideal scenario of perfect classification performance, values are reported only along the diagonal with all other values equal to zero.

Table 3. Single Energy Performance Certificates classes metrics.

Metrics	EPC Class						
	A	B	C	D	E	F	G
Precision	0.087	0.041	0.092	0.197	0.198	0.258	0.471
Recall	0.185	0.059	0.162	0.171	0.128	0.241	0.428
F1 Score	0.118	0.049	0.118	0.183	0.156	0.249	0.448

XGBClassifier Confusion Matrix

True Class	A	B	C	D	E	F	G
A	58	16	41	31	30	64	73
B	25	8	20	23	14	22	23
C	29	28	47	46	41	46	54
D	83	41	96	112	68	110	144
E	104	29	99	123	111	171	228
F	133	31	98	95	129	272	369
G	234	41	108	139	169	370	793
	A	B	C	D	E	F	G

Predicted Class

Figure 7. Model confusion matrix.

Overall, we can observe how the model shows better performances in the classification of the EPC class G, whereas performances for other classes are worse. These results clearly indicate that the unbalanced sample affect the results of the model. However, improvements compared to the Gaussian Naive Bayes Classifier are relevant and suggest that potential further improvements are possible.

2.3. Discussion

EPCs are an important element in the EU's efforts to reduce greenhouse gas emissions and improve energy efficiency, and they play a crucial role in promoting a more sustainable building stock. Data regarding EPCs, however, are scarce or data are spread across multiple databases that may be neither publicly available nor geographically complete. Thus, finding a reliable and automated approach to collect data regarding EPCs is getting more and more important. In particular if this approach is also economically feasible for covering large regions or the entire EU.

In this case study, we explored the possibility to classify building EPCs using remote sensing data. In particular, we used multispectral satellite images from Copernicus Sentinel 2, buildings footprints from Open Street Map, and air temperature data from ERA5 datasets. All these data sources are open source and freely available.

Although obtained results are not excellent, we can observe a relevant improvement compared to the baseline scores obtained at chance level. These results provide a first indication that the classification of building EPCs from multispectral satellite images is possible. However, the current approach presents several limitations. In particular, satellite images available for this case study had a resolution of only 10m. This resolution is too low for detecting details about the characteristics and elements of the buildings. Images with a much higher spatial definition are required to achieve better results. Moreover, a larger number of data is required to mitigate the issues related to class imbalance and allow the use of deep learning models (e.g., neural networks) for the classification of EPCs. Finally, the integration of other data sources regarding, for example, energy consumptions and installed systems (e.g., photovoltaic panels) may provide additional useful information for the classification of EPCs.



This approach is still at its initial phases and further improvements are required to overcome the current limitations. Nevertheless, the use of satellite images has a clear potential to provide an efficient and cost-effective method for assessing the energy performance of buildings on a large scale.

2.3.1. Quantify Economical Feasibility

In terms of economic feasibility, all data sources used in this case study are open source and freely available. This would drastically reduce the costs required to apply this approach to the whole Europe. However, there are several issues to take into account.

- Sentinel 2 images spatial resolution is limited to 10m. The use of images with higher spatial resolution is required to improve the results, but these may be no longer freely available.
- Open Street Maps data do not cover all the EU with the same quality. Further data may be needed to cover regions where Open Street Maps data is missing or not reliable.
- Several data pre-processing steps are required to obtain the right data format to be used by the model. Although these steps can be automatized to a large extent, they still require the control of experts to ensure the quality and solve eventual issues.
- Generalizability of machine learning models is usually very limited. Applying a model trained using data from one region to a completely new region can lead to sub-optimal results. Further training is usually required for the model to obtain optimal results in new contexts. In these cases new training data sets regarding building EPCs are required.

The current case study required 4 person months for the collection of data and creation of the model. This work effort can be quantified in 20'000 € (5'000 €/month for 4 months). Considering the resources already available and the limits listed above, applying the same approach to a new region is estimated to require between 1.5 and 2 person months. This work effort can be quantified in 7'500 – 10'000 €.



3. Case Study II: Photovoltaic Data Extraction from Aerial Imagery

Urbanization has been identified as the main cause of the significant changes in the Earth's climate over time. According to UN-Habitat in 2014, cities and urban areas are responsible for 78% of energy used and 60% of the carbon dioxide and greenhouse gases emitted globally. Cities have low capacity to mitigate and adapt to such changes, and this puts vulnerable populations, especially in developing countries, at risk. This endangers urban infrastructures and threatens the lives of millions of people worldwide [34].

Around half of the world's population currently resides in cities, where 80% of the nation's gross domestic product is produced. By the middle of this century, that number is anticipated to increase to two-thirds. Numerous authors, planners and architects affirm that cities play a leading role in controlling sustainability [34].

In this regard, cities must make a significant contribution to the decarbonization of the energy sector in order to meet the Paris Agreement's objectives of limiting global temperature rise to 2 °C. To aid in the shift to green energy, an increasing number of cities, mostly in the European Union (EU) and North America, have established renewable energy goals [35].

An increasing significance is given to public policies related to the exploitation of renewable energy through solar energy as a major lever for energy transition. EU countries have agreed on a new 2030 Framework for climate and energy, including EU-wide targets and policy objectives to meet by 2030. One of the targets involves reaching at least a 27% share of renewable energy consumption [36].

Solar photovoltaic (PV) had the first (36%) highest growth rates among RES over the past 30 years, respectively. The International Energy Agency (IEA) projects that by 2030, with an average annual growth rate of 13%, PVs will have met nearly one-third of the additional demand for energy [37].

One of the main options for generating energy is through distributed rooftop systems, which make up 40% of the market share in 2020. This technology is particularly useful in the built environment, especially when photovoltaic systems are fully integrated into building facades and roofs. This integration allows for the surfaces to serve a dual purpose as both energy producers and building cladding. The benefits of building-integrated photovoltaics (BIPV) and solar thermal (BIST) are numerous, including the ability to turn unused surfaces into active energy generators, reducing losses associated with electricity transmission and distribution, and providing greater energy flexibility during extreme weather conditions. In Europe, BIPV had a cumulative installed capacity of 6.9 GW_p by the end of 2019 [38].

The use of photovoltaics (PV) is crucial for reducing carbon emissions in our energy system; it is gaining more government support globally as a mean of achieving sustainable energy transformation and addressing climate change. During 2020, the solar market in the European Union (EU) experienced an expansion of 18 GW capacity installed, making solar energy the source of approximately 5.2% of the EU's overall electricity production [39]. Solar power is an economical, environmental-friendly, and adaptable energy source. In the past ten years, the cost of solar energy has decreased by about 82%, making it the most cost-effective electricity option in several regions of the EU [39]. Over time, the development of solar PV technology has significantly improved thanks to technological advancements, reduced material costs, and global push for electricity generation from renewable sources. As a result, the utilization of solar PV technology has substantially increased.



One issue with the quick growth of solar PV, however, is the monitoring and mapping of their installations. PV systems are primarily smaller in scale and installed on rooftops by individual owners, in contrast to other electricity generation technologies such as coal, gas, or wind power plants. The decreasing cost of PV systems and the subsequent rapid increase in the use of this technology have presented a challenge for monitoring all the installations due to their decentralized nature and large quantity [40].

According to various sources, solar PV and the energy they produce are not appropriately recorded or tracked in a centralized database; the information about the distribution of solar PV installations can vary considerably from country to country. Obtaining geospatially precise information on rooftop PV for localized regions like towns and counties presents a significant challenge. Traditional methods, such as surveys and utility company data logs, are not suitable for this purpose as they are burdensome and yield insufficient data for the desired level of precision [41]. Additionally, data estimated with these methods quickly become outdated due to the rapid growth of rooftop PV; costly and periodic data collections are necessary to keep the data current.

One way to keep track of installed PV systems is by gathering data through self-reports, like the 'Tracking the Sun' project [42] and Germany's official PV registry [43]. These registries can be customized to collect specific information about the PV systems, including ownership. However, manual data collection can be time-consuming and prone to human error. Moreover, PV systems are often registered by street address, which may not always accurately reflect the system's actual location. There are situations where network operators keep records of the precise locations and capacities of all solar PV systems that are connected to their networks. Despite this, there is a possibility that a portion of systems are not recorded or are inadequately logged, or that omissions in the registry may occur. Also, in certain cases, network operators may decline or be unable to disclose these data to external parties [44], [45]. A Dutch study reported a discrepancy of about 25% between registered and unregistered PV installations in several residential areas of the country [46].

The adoption of solar PV in off-grid settings is also increasing significantly. Such systems are unlikely to be recorded with a centralized entity, and yet it would be beneficial to acknowledge their existence to monitor the overall expansion of solar PV in a given area.

The above issues raise a need for a new approach to obtaining rooftop PV information.

Monitoring PV installations is important to a variety of stakeholders and applications. For instance, utility enterprises necessitate PV databases to execute long-term capacity planning for electricity networks. Governments and policy makers depend on current and reliable PV database to formulate, monitor, and evaluate energy policies related to PV adoption. Knowledge of accurate PV data is an asset to making educated choices when determining energy policies and regulations, planning for capacity expansion, upgrading transmission and distribution systems, and making operational decisions to maintain grid reliability and resilience. Researchers as well benefit from updated data when developing innovative solutions in the PV field [44], [47].

Another value of PV monitoring is the use of the data for the purpose of urban planning, which is the area of interest of this research project. The study of the distribution of PV in a city can provide valuable insights to urban planners. By analysing the location and density of PV installations, they can identify areas with high potential for solar energy generation and incorporate this information into their planning decisions. For example, they can prioritize the development of solar-friendly building codes and zoning regulations, encourage the installation of PV systems in public buildings and spaces, and promote the use of solar energy in transportation systems. This can help to reduce the city's carbon footprint, increase energy efficiency, and improve the overall sustainability of the urban



environment. Additionally, the study of PV distribution can help urban planners to identify areas that are vulnerable to power outages and develop strategies to improve grid resilience and reliability [48], [49].

3.1. Methodology

3.1.1. Detection of Rooftop Mounted Photovoltaic Installations from Aerial Imagery

Object detection from aerial imagery has been investigated extensively over the last decade however, the detection of solar panels has been unexplored until very recent years. Several promising methods have emerged so far, although the use of satellite and aerial imagery for identifying solar PV systems is still a developing field of research. Malof et al. [50] have made significant advancements in two types of approaches. Initially, they employed a support vector machine for object detection using standard pixel-wise feature extraction and classification. Later, they replaced the support vector machine with a random forest classifier to assign probabilities to each pixel, enabling segmentation. Their research progressed to the use of a convolutional neural network with convolutional and max-pooling layers for further development [41].

Overall, literature on this subject has focused primarily on two detection algorithms, Random Forest (RF) Classifiers [51] and Convolutional Neural Networks - CNN [50], both of which have been effective in image recognition tasks. While both approaches have proven successful, Convolutional Neural Networks have outperformed other methods on significant image recognition benchmarks in recent years. Nevertheless, the time required to train CNNs is often substantially greater than that of other competing algorithms, such as RF. Furthermore, the process of designing CNNs is challenging, and numerous models may require extensive testing [45]. DeepSolar is a noteworthy study that made significant progress in this field by training on more than 350,000 images, achieving a 90% precision and recall for detecting solar panels and a mean relative error of 2.1% for estimating their size. However, their methodology demands a substantial quantity of image data and computational power, making it only accessible to organizations with sufficient resources [40].

In present study, the process of detection of photovoltaic installations is carried out in a GIS environment (please see Figure 8). The software of choice is GRASS GIS, in which a variety of works of object-based classification and image segmentation has been carried out and properly documented [52], [53].

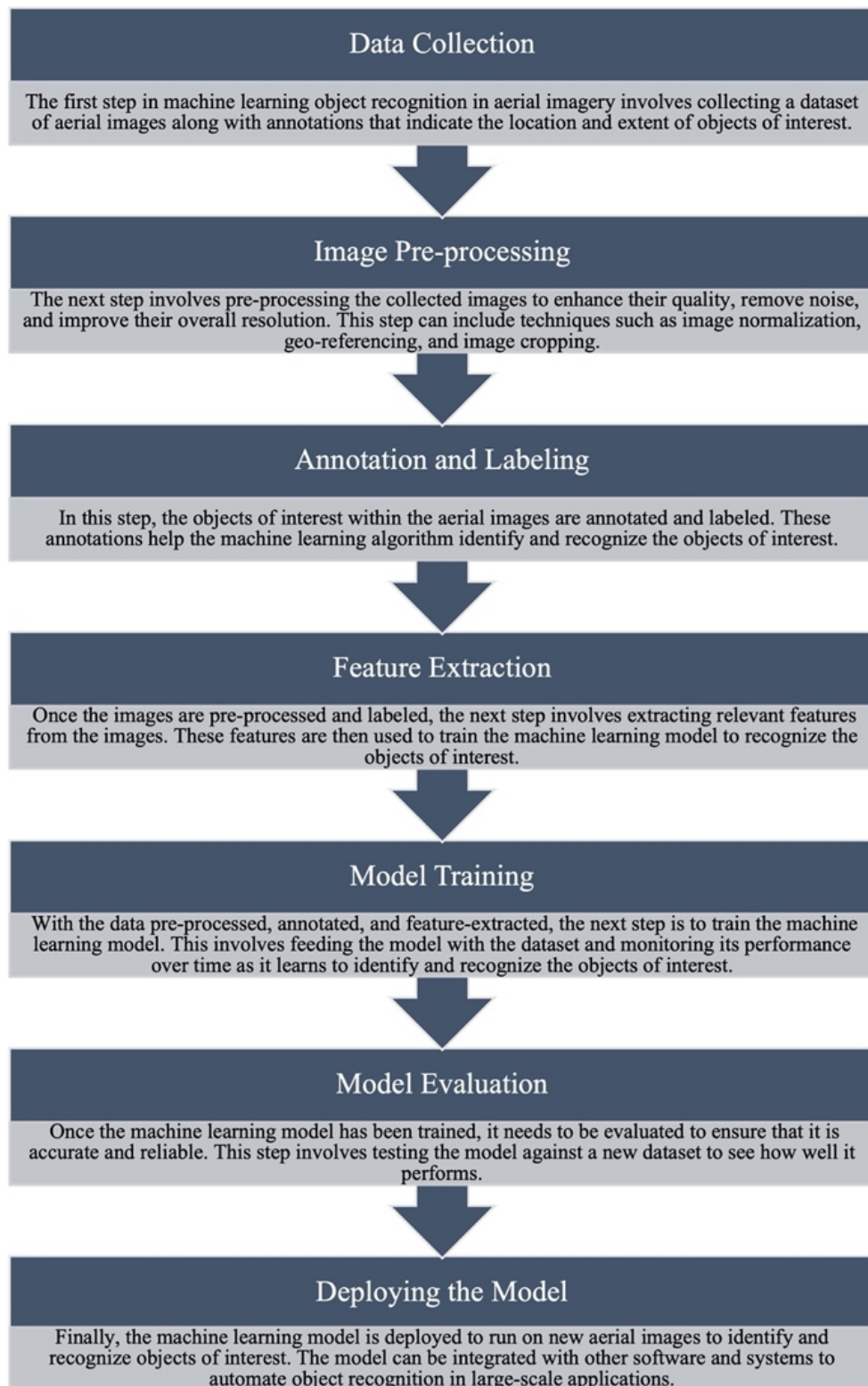


Figure 8. Steps for the application of machine learning techniques on imagery. Source: Author's elaboration based on Ng et al. [54].

3.1.2. Capacity Estimation of Detected Photovoltaic Installations

The calculation of the capacity of a photovoltaic installation can be computed when the surface area of the installation is known.

As of 2022, on average, photovoltaic modules on the market have an efficiency ranging between 15% and 20% [43].

The capacity, expressed in kW_p , is then calculated as indicated in Equation (4).

$$Capacity (kW_p) = PVArea \times 0.15 \text{ to } 0.20 \quad (4)$$

The result is presented as a range, depending on the efficiency of the module. This accounts for the impossibility to have data on the efficiency of single installed PV modules, relying solely on aerial imagery.

The slope of the examined photovoltaic installations poses another variable in the calculation of its exact surface area. This can be solved through the use of a Digital Surface Model (DSM) to verify the slope of the surface on which the photovoltaic modules are installed or the tilt of the photovoltaic module itself. For the conducted case study, however, no Digital Surface Model matching the aerial imagery resolution of 0.25 meters was available. A DSM of a 1-meter resolution did not allow the exact determination of the slope of the modules except for a few extensive installations. This variable can be solved by accounting, for those modules for which the slope cannot be identified, for a default slope value between 0 and 60 degrees. The optimal tilt of a photovoltaic panel depends on several factors, including location and season of the year [55]. For the purpose of this work, an average value of 30 degrees will be considered. The influence of this value does not change drastically the results of the capacity estimation, as proved by So et al. [56].

The equation for calculating the true area of an inclined PV panel, given the area detected from above, relies on trigonometry (see Equation 5). It accounts for the detected area, divided by the COSIN of the angle at which the PV panel is inclined (in this work that is 30 degrees).

$$True Area = Detected Area \times \frac{1}{\cos(30)} \quad (5)$$

3.1.3. Context

Crevillent is a Spanish town with around 29717 inhabitants as of 2021 according to the Spanish National Institute of Statistics - INE [57] (See Figure 9). It is located in the southeast of the country, in the Alicante province, and it is part of the administrative division 'Comunitat Valenciana'.

It is situated in a valley surrounded by mountain ranges, including the Sierra de Crevillente to the north and the Sierra de Cabeçó to the south. The town is located at an altitude of approximately 230 meters above sea level and covers an area of around 68 square kilometers. The town is located about 20 kilometers inland from the Mediterranean Sea and is approximately 50 kilometers south of the city of Alicante. The area surrounding Crevillent is characterized by a diverse landscape of mountains, valleys, and plateaus [58]. It has a Mediterranean climate, which is characterized by mild, rainy winters and hot, dry summers. The region is prone to droughts and heat waves during the summer months, and it is one of the driest areas of the country, averaging 285 mm of rainfall each year, against a national

average of 628 mm for the year 2019 [59]. The region presents one of the highest photovoltaic power potentials in the whole country (please see Figure 9).

Crevillent was chosen as a representative case study thanks to the access of bottom-up data provided by IVE, which served as faithful ground truth data against which the result of the work could be compared and evaluated.

Furthermore, Crevillent presents a clear distinction between a historic city centre, mostly serving the function of residential area, and new industrial districts developed in the last decades and a large extent of agricultural land plots [58].

Crevillent has plans for becoming Spain’s first energy community in loco. In this city, the inhabitants will collectively own photovoltaic panels that will generate electricity for their consumption. While the process can be long and complicated, Crevillent has a significant advantage in that nearly the entire town receives its energy from Enercoop FONT. Enercoop is distinct from the majority of Spanish energy cooperatives in that it functions as both an electricity vendor and distributor. This is uncommon in Spain, where the distribution of electricity is divided among five main companies, each operating in a specific jurisdiction [60].



Figure 9. Photovoltaic Power Potential in Spain Source: Global Solar Atlas 2.0 [59]

3.2. Application of the Methodology

3.2.1. Data

The aerial imagery used in this project is freely available as open data and has been retrieved from the portal of IDEV (Infraestructura Valenciana de Dades Espacials) [61].

The imagery consists of orthophotos in natural color (red, green, and blue - RGB) and false infrared color (IRG) covering the extent of the Comunidad Valenciana at a resolution of 25 centimeters per pixel. The images are based on a RGBI digital photogrammetric flight and were taken from 08/05/2022 to 11/06/2022. The data was downloaded in the form of six 1:5.000 sheets in a TIFF format which were then patched as a unique image in a GIS environment.

Bottom-up data on photovoltaic installations in Crevillent have been provided by Enercoop, the energy cooperative managing the electricity network of the town. The data was in the form of a list of 98 addresses with photovoltaic installations as of 2022 and the relative installed inverter capacity expressed in Watts.

3.2.2. Manual Annotation of Photovoltaic Installations

The list of addresses with photovoltaic installations was used as a source to manually locate the buildings within the aerial imagery. It has not been possible to execute a work of automated geocoding as the addresses have been provided in different formats, not recognized by web mapping platforms. Instead, addresses have been manually located using the Spanish cadaster web service [62]. Photovoltaic installations have been manually annotated by drawing vector polygons within QGIS. Polygons were drawn over groups of photovoltaic panels adjacent one to the other. As there are no plans to address individual panels or treat each panel separately, the decision was made not to draw polygons over singular panels that are installed in proximity to one another. In total, 416 polygons have been labelled within the municipality of Crevillent. The total area of photovoltaic surface annotated amounts to 20'223.8 square meters. These annotations will then be used as ground truth for the evaluation of the effectiveness of the detection model. Please see Figure 10 and Figure 11 for examples of manual annotation of PV installations.



Figure 10. Manual annotation of PV installations at the municipal stadium Source: Adapted by the author on QGIS.

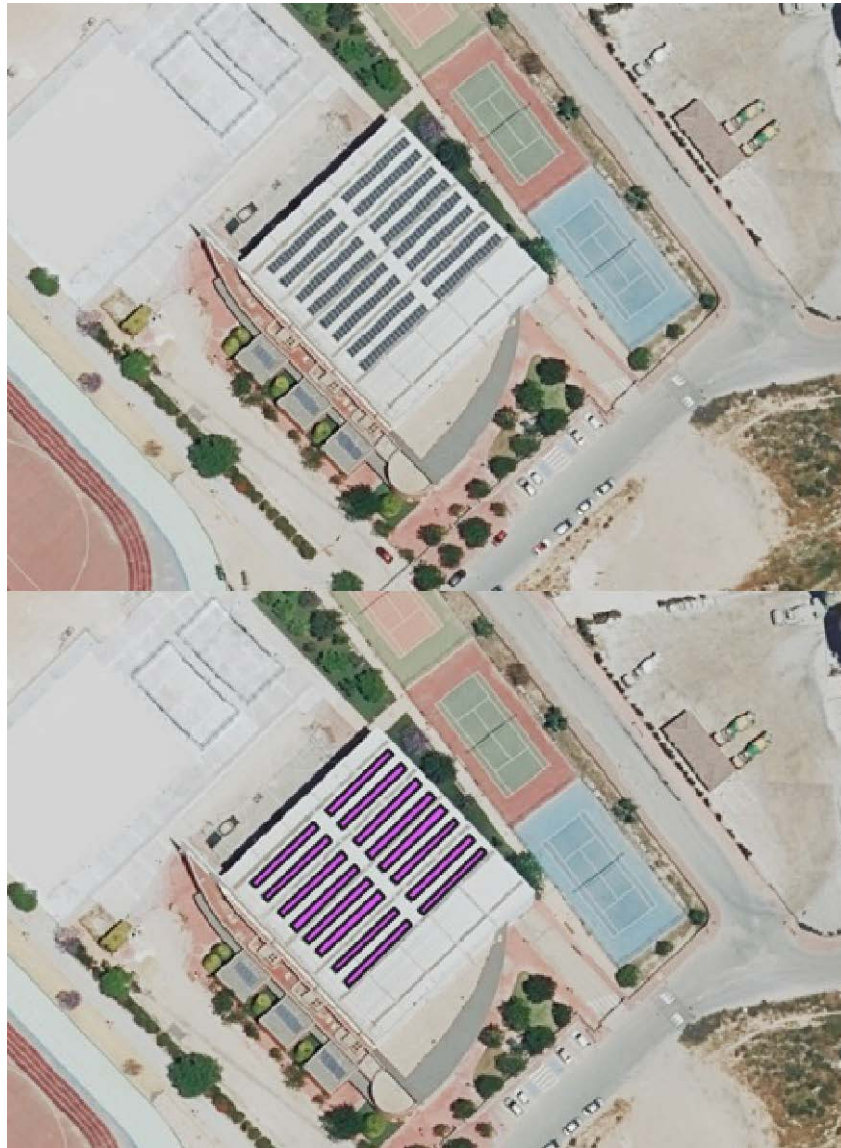


Figure 11. Manual annotation of PV installations on the roof of an industrial building Source: Adapted by the author on QGIS.

3.2.3. Image Processing

A Principal Component Analysis (PCA) has been carried out in GRASS GIS in order to obtain the definition of band statistics that best highlights the presence of photovoltaic panels. In image processing, Principal Component Analysis (PCA) is a technique used to reduce the dimensionality of image data while preserving most of the relevant information. It computes the covariance matrix of the image pixels and finds the eigenvectors and eigenvalues of the covariance matrix. The eigenvectors represent the principal components of the image, which are linear combinations of the original pixel values. The eigenvalues indicate the amount of variance in the image explained by each principal component [63].

3.2.4. Detection of Rooftop Mounted Photovoltaic Installations from Aerial Imagery

In order to obtain a better result in the automatic recognition of photovoltaic panels, it was decided to operate only on roof mounted photovoltaic installations, avoiding a large number of ground elements that could be recognized by the algorithm as false positives. This approach has been adopted in previous works for the same operative reasons; rooftop mounted installation the vast majority in cities and towns, due to the scarce amount of ground space available [45], [64]. This step also allowed to drastically reduce computational resources needed by the software to run the machine learning algorithms. This choice was made after researching and verifying the absence of large-scale ground mounted photovoltaic plants within the territory of Crevillent. Data about the footprint of buildings within the municipality of Crevillent has been downloaded from the spatial database of the Generalitat Valenciana IDEV (Infraestructura de datos Espaciales Valenciana). The downloaded data is at a scale of 1:5'000 and it was last updated in January 2023 [65].

Due to a tilt in the aerial imagery at disposal, a portion of the facades of buildings was visible and it represented an obstacle for the automatic detection of objects, as it was included in the vectorial polygons recognized as buildings. To overcome this issue, an operation of orthorectification has been carried out. Orthorectification is a process of removing the distortions present in remotely sensed imagery and converting it into an accurate, corrected, and georeferenced image that can be used for mapping and analysis purposes [66].

The process involved the identification of the exact location of the three cameras from which the three different orthophotos composing the municipality of Crevillent had been taken. Then, three buildings were selected, serving as ground control points. The three different orthophotos were then overlapped. This allowed the manual reconstruction of the seamlines composing the mosaic of the pictures, by finding areas where there were large differences between the adjacent images. Seamlines are the boundaries between adjacent image strips that are mosaicked together to create a larger, seamless image.

Once the seamlines dividing the three pictures have been delineated, it was possible to exclude the facades from the vectorial footprints of buildings (please see Figure 12).

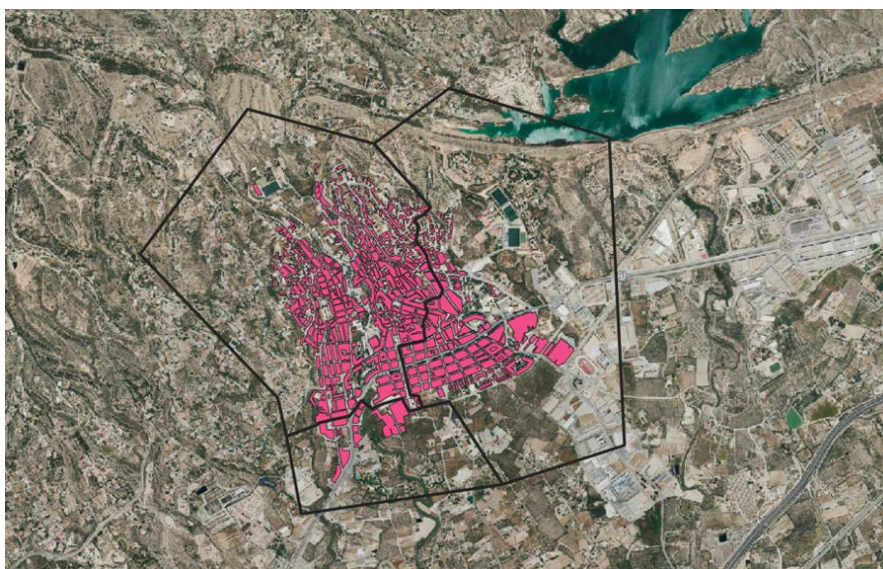


Figure 12. Seamlines detected within Crevillent Source: Adapted by the author on QGIS.



The detection of photovoltaic panels has been carried out through techniques of machine learning, using the function `r.learn.ml` in GRASS GIS. This function allows to perform supervised classification and regression of GRASS rasters using the python scikit-learn package [67].

To train the model, two classes of images have been used: one with photovoltaic installations and the other one with roofs. 60 images were randomly selected for each of these two classes. Training images of photovoltaic panels were created by randomly selecting photovoltaic installations and drawing polygons over them, as well as selecting smaller sections from various photovoltaic installations.

The choice to use traditional machine learning methods rather than deep learning methods (e.g., CNN) was taken due to the extensive training required for the latter, in favor of a more immediate approach in line with the scope and resources of the project.

Several classification and regression methods are available within the `r.learn.ml` function. Due to the relatively small number of training images and modest size of the area to be analyzed, a technique of logistic regression has been chosen over other methods like random forest classifier. Logistic regression is part of the Generalized Linear Model (GLM) family and if used specifically to model the probability of a binary or categorical outcome based on one or more predictor variables. It assumes that the relationship between the predictor variables and the outcome is linear in the transformed space and can be represented by a logistic function. Logistic regression is a simple and interpretable algorithm that can be used for both small and large datasets, and it works well when the relationship between the predictors and the outcome is linear or when the data is not too complex. However, it may not work well when the relationship between the predictors and the outcome is non-linear or when there are interactions between the predictors [68].

Random forest classifier, on the other hand, is a non-linear ensemble model that combines multiple decision trees to classify data. It works by randomly selecting subsets of the data and the predictors to build each decision tree, and then aggregating the results of the trees to make a final prediction. Random forest is a powerful algorithm that can handle non-linear relationships, interactions between predictors, and high-dimensional data. It is also less prone to overfitting than a single decision tree. However, random forest can be more complex and harder to interpret than logistic regression, and it may not perform well on small datasets or datasets with imbalanced classes [69].

The next step consisted in using the `r.neighbors` function within GRASS GIS in order to obtain more homogeneous results, filling gaps in areas markedly recognized as photovoltaic panels as well as filtering out single pixels or very small patches which can be considered as outliers. In GRASS GIS, the `r.neighbors` function is used to perform a neighborhood operation on a raster map layer. The function calculates a new value for each cell in a raster map based on the values of its neighboring cells within a specified window size [70].

3.3. Results

3.3.1. Detection of Rooftop Mounted Photovoltaic Installations from Aerial Imagery

The results of the logistic regression are compared against the manual annotations of photovoltaic installations used as ground truth. Figures 11, 12, 13 show specific examples of how the prediction model compared to the ground truth. The performance of the model is measured by Mean Intersection over Union (mIoU), which measures the number of pixels common between the ground truth and prediction masks divided by the total number of pixels present across both masks.

Intersection Over Union (IoU) is a number that quantifies the degree of overlap between two boxes. In the case of object detection and segmentation, IoU evaluates the overlap of the Ground Truth and Prediction region [71].

The model used for identifying photovoltaic installations achieved a mIoU of 0.67.

The result obtained with a logistic regression in this case study does not achieve the accuracy of more complex object detection models, scoring > 0.95 . However, it can be still considered satisfactory for the purpose of this work considering the relatively low training required and low amount of input data needed. Please see Figure 13, Figure 14, and Figure 15 for examples of results of logistic regression in detecting photovoltaic installations.

It can also be considered as an aid for manual data collection concerning photovoltaic installations, which remains costly and time consuming.

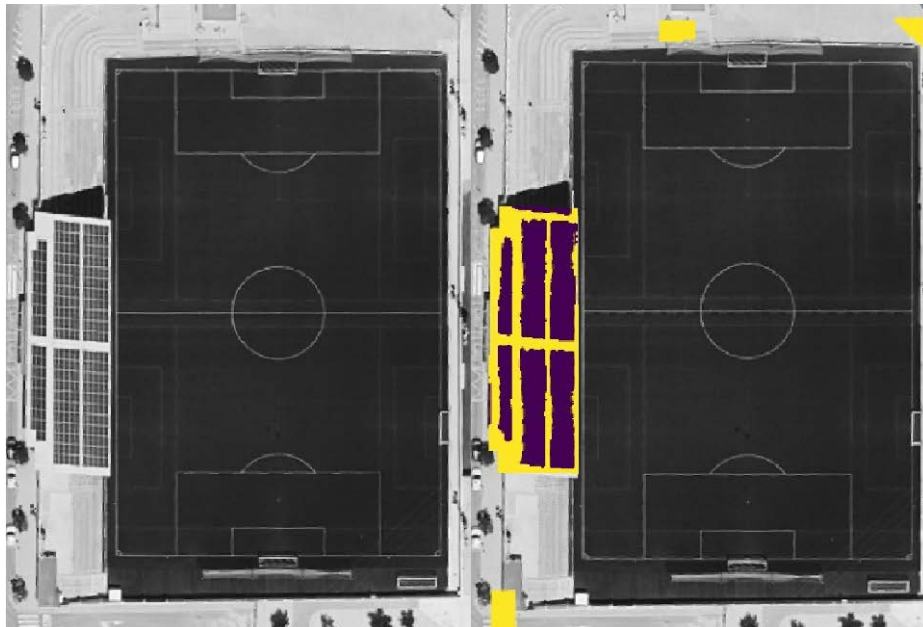


Figure 13. Examples of results of logistic regression in detecting photovoltaic installations. Source: Adapted by the author on GRASS GIS.

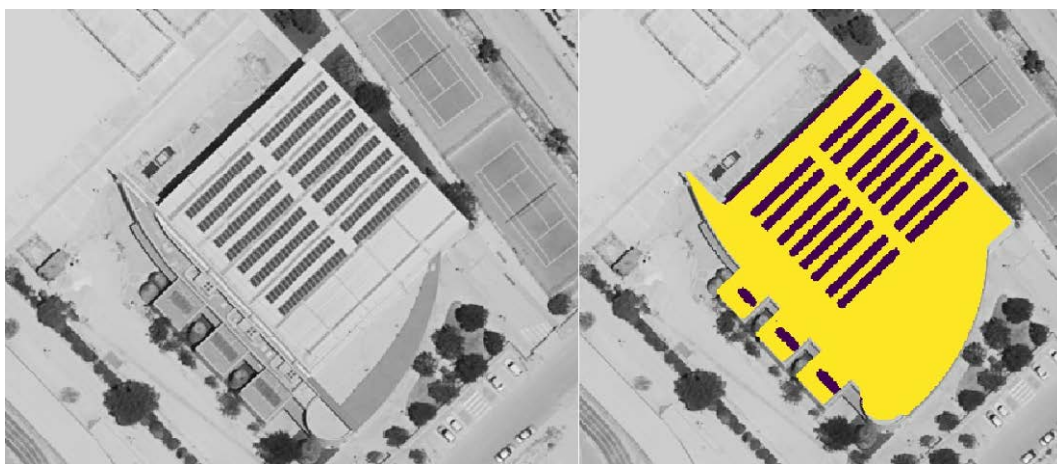


Figure 14. Examples of results of logistic regression in detecting photovoltaic installations. Source: Adapted by the author on GRASS GIS.

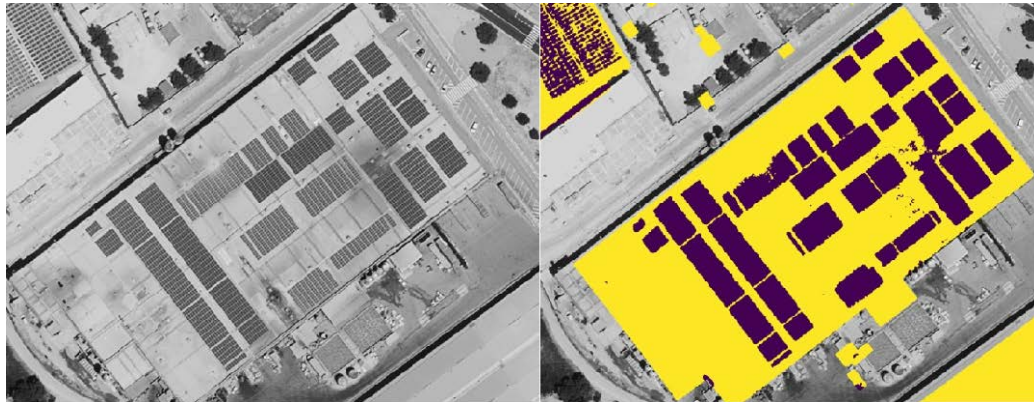


Figure 15. Examples of results of logistic regression in detecting photovoltaic installations. Source: Adapted by the author on GRASS GIS.

3.3.2. Capacity Estimation of Detected Photovoltaic Installations

Concerning the estimation of the capacity of each photovoltaic installation address, the meter of comparison of the success of the calculations was the list of addresses reporting the PV capacity expressed in kW_p for 98 addresses in Crevillent. The list was provided by Enercoop to serve as ground truth data against the model.

The results of the calculations consist of a range, considering a panel efficiency between 0.15 and 0.20. Overall, 58 out of the 98 addresses fit within the calculated kW_p range.

An example of the calculation process for one address with declared capacity of 10'000 Watts is reported below (please see Figure 16). The logistic regression found the two separated photovoltaic installations and attributed to them surface areas of 29.1 square meters and 21.3 square meters for a total surface area of 50.4 square meters.

$$29.1 \text{ m}^2 + 21.3 \text{ m}^2 = 50.4 \text{ m}^2$$

The slope of the roof, and therefore the slope of the photovoltaic installations cannot be determined using the Digital Surface Model. As a consequence, a range between 0 and 30 degrees of slope are attributed to the surface. In case the surface was at an angle of 30 degrees the following formula is used:

$$\text{True Area} = \text{Detected Area} \times \frac{1}{\cos(30)} \tag{6}$$

$$\text{True Area} = 50.4 \text{ m}^2 \times 0.866 = 58.19 \text{ m}^2$$

In the example, the real area of the panel tilted at an angle of 30 degrees would be 58,19 square meters.



Figure 16. Example of detection of a photovoltaic installations Source: Adapted by the author on GRASS GIS.

The range of capacity is then calculated as follows:

$$\text{Minimum Value: } 58.19 \times 0.15 = 8.72 \text{ kW}_p$$

$$\text{Maximum Value: } 58.19 \times 0.20 = 11.64 \text{ kW}_p$$

The correct value provided of 10'000 Watts falls within the calculated range.

3.4. Discussion

The main advantage of the adopted methodology is that it requires relatively low effort in training. This is particularly useful in situations with a limited availability of data or resources.

Although aerial imagery has proven to be effective in accurately identifying buildings, vehicles, and roads, solar PV systems present a unique set of characteristics that pose challenges to their identification. This section outlines the main challenges that have been encountered the work and that have been common to related research on the topic.

Solar PV systems can be easily mistaken for various objects that share similar visual characteristics. These objects may include solar hot water systems, skylights, edges of houses, cables, and even swimming pools. Performing the image detection only on roofs limits possible error sources, such as vehicles windscreens and swimming pools, but the issue still persists to a certain extent [44].



False negatives present another challenge in the development of this typology of project. Solar PV systems can present a significant identification challenge, even for experienced human annotators, in various situations. For instance, this may occur when black panels are installed on black rooftops, especially when the image resolution is inadequate. Difficulties in identifying such systems even by manual annotators can result in lower quality of training sets, leading to less precise classification or segmentation. Additionally, small, or atypically configured solar PV systems, which are not rare on residential rooftops, can be particularly challenging to identify. A similar issue is presented by new technologies that integrate photovoltaic installations in materials and styles developed to be less visible as possible, rejecting the common style of photovoltaic panels in favour of tiles and wall mounted installations [44].

One other aspect that can pose a challenge to an immediate replicability of the work is the heterogeneity in the availability of high-resolution aerial imagery depending on the local operational context.

3.4.1. Quantify Economical Feasibility

The aerial imagery used for this case study is available as open data from the web GIS portal of the Comunidad Valenciana, while the list of addresses with PV installations that served as ground truth data is restricted and it was shared privately by Enercoop. Ortophotos at a resolution of 0.25 meters are available for several areas of the European Union but not for its entirety. Therefore, this aspect can be a limit for the replicability of the work. Scaling up a machine learning model requires a proportional training, in order to obtain acceptable results.

The current case study required 6 person months for the collection of data and creation of the model. This work effort can be quantified in 30'000 € (5'000 €/month for 6 months). Considering the resources already available and the limits listed above, applying the same approach to a new region is estimated to require between 5 and 6 person months. This work effort can be quantified in 25'000 – 30'000 €.

4. Case Study III: Analysis Photovoltaic Distribution in Relation to Urban Morphology from Aerial Imagery

Building detection from aerial imagery has become increasingly important in recent years due to the abundance of high-resolution satellite imagery and the need for accurate and up-to-date urban planning information.

Building detection algorithms typically involve the use of machine learning techniques, such as convolutional neural networks (CNNs) or support vector machines (SVMs), to analyse satellite imagery and identify areas that correspond to buildings. These algorithms can be trained on large datasets of labelled satellite imagery, where each pixel in the image is labelled as either belonging to a building or not. The algorithm then uses this training data to learn patterns and features that are associated with building locations, such as the size and shape of rooftops, the presence of windows or other architectural features, and the overall texture and colour of the building [72]. Once the algorithm has been trained, it can be used to analyse new satellite imagery and automatically detect buildings in the image. This can be done on a pixel-by-pixel basis, where each pixel in the image is classified as either belonging to a building or not, or by analysing larger patches of the image to identify complete building structures. The resulting outputs can be used to create detailed maps of building footprints and their associated attributes, such as height, orientation, and construction materials [72].

The automatic detection of buildings allows for multiple possibilities of use. If the detected buildings can be compared with official registries, a report of illegal constructions can be produced and consequential actions and policies can be implemented. In the field of urban planning, automatic detection of buildings from aerial imagery can help in identifying the built-up areas, their distribution, and changes over time. This information can be useful for urban planning, land use management, and zoning. After natural disasters, automatic building detection from satellite images can help assess the extent of damage caused by natural disasters like earthquakes, floods, or hurricanes. This information can be critical for rescue and relief operations. Automatic building detection can also help monitor changes in natural resources, such as forest cover or wetlands, by identifying new buildings or land use changes. Finally, automatic building detection can assist with population mapping, estimating population density, and identifying urban and rural areas.

4.1. Methodology

For the purpose of this work, the detection of buildings is carried out using the Mapflow software. The software is run as a plugin within QGIS. Mapflow is an AI-mapping platform that uses machine learning models to detect and extract features from satellite and aerial images. It can extract the roofprints of buildings from high-resolution imagery with reportedly high accuracy [73], [74].

A normalized Digital Surface Model (nDSM) of the province of Alicante from the year 2016 has been downloaded from the Geoportal of the Comunitat Valenciana [75]. The nDSM is then joined with the vector layer of the buildings recognized with the Mapflow service. This passage links the footprint of buildings with their height. The height of the building is calculated as an average of the measure of all the points within the building shape.

A spatial join command finally allows to link the buildings with the photovoltaic installations.

Information concerning the land use of the area is obtained from the Municipal Plan of the city, dividing the territory in three main categories: residential, industrial and agricultural/rural. In order to operate within an urban context and calculate plausible and comparable measures of urban density

and form, non-urban land (agricultural areas, big parks, rivers) is discarded from calculation, leaving residential and industrial areas as the two typologies urban form to study. In the context of Crevillent, residential areas present a dense fabric, tall buildings and few open spaces. On the contrary, industrial areas presents a low-density urbanization characterized by two storey's tall buildings in average and by generous open spaces (see Figure 17 and Figure 18).



Figure 17. Examples of results of detection of buildings from aerial imagery using Mapflow. Source: Author's elaboration on QGIS.

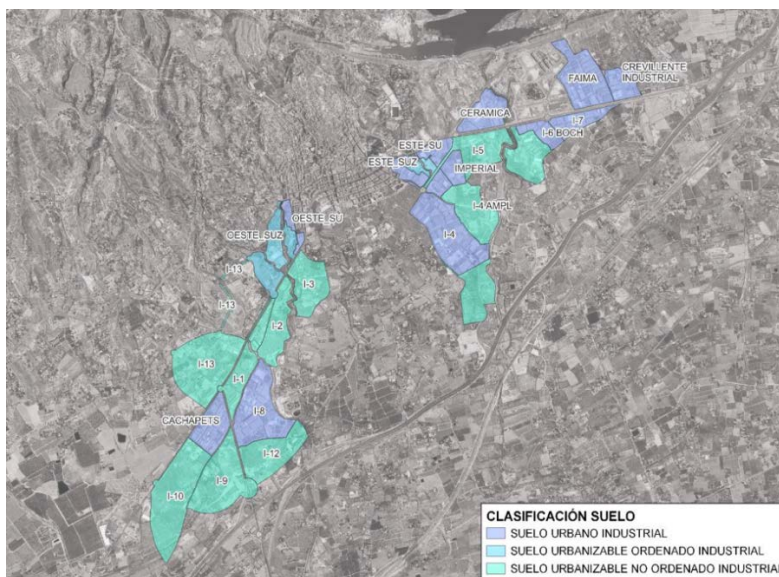


Figure 18. Industrial polygons of Crevillent Source: Plan Municipal, Ayuntamiento de Crevillent.

For the purpose of this work, a list of addresses with photovoltaic installations in the city of Crevillent, Spain, has been used. The PV installations have been manually located and their area has been calculated. The objective of this case study is to investigate the relationship between urban residential and industrial areas with respect to presence of PV installations. Data acquired with machine learning technology and existing bottom-up data are used together to analyse land use and typology of the buildings for PV installations, and to identify tendencies and patterns in the use of PV technology across the territory.



4.2. Results

The analysis of the distribution of photovoltaic installations put in relation different variables.

- Land use of the area, either residential or industrial
- Number of buildings with photovoltaic installations
- Total area of photovoltaic installations
- Height of buildings with photovoltaic installations
- Area of roofs hosting photovoltaic installations

The main residential area hosting rooftop mounted photovoltaic installations is the historical city center of Crevillent. The more recent residential area of San Felipe Neri also presents 4 buildings with photovoltaic installations.

The center presents the largest number of buildings with photovoltaic installations, 15, but it also hosts one of the lowest areas of photovoltaic installations. This element testifies a high degree of fragmentation of roofs in the city center as opposed to industrial areas.

The surface of photovoltaic installations in residential areas is 520 square meters, distributed over 19 different buildings. This value is extremely small if compared with the surface of photovoltaic installations present in industrial areas: 18424 square meters, distributed over 35 different buildings (please see Figure 19 and Figure 20).

In fact, the average area of a residential roof hosting PV installations is 2017 square meters, lower than the 3953,6 square meters characterizing the average industrial roof with PV presence (please see Figure 21).

The height of the buildings hosting PV installation reflects the characteristic forms of the land use of interest. The average height of buildings with PV installations in residential areas, notoriously more dense, is 9'193 meters, while industrial buildings average 7'755 meters (please see Figure 22).



Figure 19. Number of buildings with PV installation per zone. Scale 1:40000. Source: Adapted by the author on QGIS



Figure 20. Area of PV installation per zone. Scale 1:40000. Source: Adapted by the author on QGIS.



Figure 21. Average Area Roofs with PV installations per zone. Scale 1:40000. Source: Adapted by the author on QGIS.



Figure 22. Average height of buildings with PV installations per zone. Scale 1:40'000. Source: Adapted by the author on QGIS.

4.3. Discussion

The results obtained in this case study reflect the relationship between urban morphology, in particular urban density, and photovoltaic installations that emerge from literature on the topic. The larger amount of photovoltaic surface is present in industrial areas connotated by lower building density.

Poon et al. [76] also found that urban morphology on the neighbourhood scale has a significant impact on electricity generation by photovoltaic panels that are installed on building rooftops and facades. However, the study also noted that morphological studies cannot provide replicable, transposable model types as each city is not identical.

The most effective way to evaluate the impact of urban morphology on rooftop solar potential is through a city-scale approach that takes into account the building footprint and shading patterns. Boccalatte et al. [77] used Geneva GIS data to evaluate the impact of urban morphology on rooftop solar radiation. The study mapped the proportion of the tessellation cell covered by the building footprint, which allowed for a precise mapping of the densest areas within the urban fabric.

If the development of solar energy is particularly important in cities, main consumers of energy demand, dense areas limit the incoming sunlight and the deployment of urban solar power plants. City centers present a more difficult environment for the expansion of photovoltaics, as building roofs are often of complex structure and split into numerous roof sections [78]. Largest roofs within dense urban tissues can often be found on public and service buildings.

While the compact city model is preferable to a less dense setting, since it permits synergies and green policies that require minimum population densities, it has been demonstrated how density impacts potential for passive solar architecture [78].

Because of its focus on the urban environment, the case study has not included rural areas of the territory; therefore, a share of PV installations was neglected. A future study may want to encompass rural areas as well for a more complete analysis.

4.3.1. Quantify Economical Feasibility

The aerial imagery used for this case study is available as open data from the web GIS portal of the Comunidad Valenciana, while the list of addresses with PV installations that served as ground truth data is restricted and it was shared privately by Enercoop. Orthophotos at a resolution of 0.25 meters are available for several areas of the European Union but not for its entirety. Therefore, this aspect can be a limit for the replicability of the work. However, building detection can be performed with successful results even if using satellite images, therefore opening the way for replications of the work at different scales.

Scaling up a machine learning model requires a proportional training, in order to obtain acceptable results.

The current case study required 1 person months for the collection of data and creation of the model. This work effort can be quantified in 5'000 € (5'000 €/month for 1 month). Considering the resources already available and the limits mentioned above, applying the same approach to a new region is estimated to require between 1 and 2 person months. This work effort can be quantified in 5'000 – 10'000 €.

5. Conclusions

The building sector plays a crucial role in the achievement of the European climate neutrality by 2050. In fact, the building sector accounts for 36% of global energy use and 37% of energy-related GHG emissions. For these reasons, effective policy initiatives and directives aimed at reducing greenhouse gas emissions, promoting sustainable energy use, and improving energy efficiency in the building sector are fundamental.

However, to inform policy makers decisions, accurate and reliable data on the building stock are essential. Precise and accurate information are needed by policymakers to monitor the current state of the building stock and obtain useful insights regarding its future development. In this way, they can develop tailored measures to obtain the best improvements.

There are two main approaches for the collection of data regarding the building stock: the top-down approach and the bottom-up approach. Data obtained through top-down approaches are useful to analyse building stock dynamics and broad patterns on a larger scale, however, they lack the required granularity for implementing specialized strategies is significantly hindered. On the contrary, bottom-up approach allow to collect very detailed information but is extremely time-consuming and expensive.

Remote sensing can become an ideal data source to overcome these limits. Remote sensing can provide reliable and detailed information in an automated and economically feasible way. Application of remote sensing in the collection of data regarding the building stock are scarce in the scientific literature but results are promising.

In this Deliverable, we presented three case studies based on remote sensing data for the analysis of different aspects of the building stock. Accuracy and reliability of the proposed approaches were evaluated as well as their economic feasibility.

In the first case study, we propose a methodology for automatically classifying building EPCs based on the analysis of satellite images. Although there are several limits, obtained results provide a first indication of the potential of using satellite images for the classification of EPCs. This approach is still at its initial phases and further improvements are required. However, this approach has the potential to provide an efficient and cost-effective method for assessing the energy performance of buildings on a large scale.

In the second case study, we present an approach based on aerial images to detect installed photovoltaic panels and estimate the installed photovoltaic capacity on rooftops in urban areas. The first part of the work focused on the automatic detection of rooftop mounted photovoltaic installations using logistic regression within GRASS GIS. This method was chosen for its low training requirements compared to more complex algorithms. The validation method of Intersection over Union achieved a score of 0.67 based on a list of addresses with PV installations serving as ground truth data. The result does not provide an accuracy as high as other algorithms, but the low amount of training required justifies the choice of the method. In the second part of the project a methodology was developed for calculating the installed PV capacity using the area of the detected PV installations. To account for the tilt of the PV panels, a first step consisted in finding the true area of the installations, and then an efficiency value of 0.15 to 0.20 was used to create a range of results. A list of addresses with reported installed capacity served as ground truth data; 58 out 98 of these addresses fit within the calculated range.



Following this approach, large scale area can be evaluated, and results could provide valuable information for urban planners and policymakers in promoting renewable energy adoption.

The third part of the work focused on an analysis of the distribution of PV installations in industrial and residential areas. First, footprints of buildings were detected by machine using a GIS plugin and integrated with the existing rooftop PV installations. Then, the vectorial data was merged with a normalized Digital Surface Model and with bottom-up information on the land use. This led to the analysis of different variables: land use of the area, either residential or industrial; number of buildings with PV installations; total area of PV installations; height of buildings with PV installations and square footage of roofs hosting PV installations.

The analysis revealed that a large majority of PV surfaces is located in industrial areas. Residential roofs present a higher degree of fragmentation in the installations, with 19 different buildings presenting PV installations for a total area of 520 square meters versus 18,424 square meters over 35 different buildings in industrial areas. Industrial areas also host PV installations on lower buildings compared to residential areas, which are characterized by denser urban fabrics.

Overall, the results obtained from the three case studies provide a clear hint on the potential of using remote sensing for the collection of data regarding the European building stock. Remote sensing can provide reliable and detailed information in an automated and economically feasible way. However, remote sensing is still in its initial stages of development and further research is required to fully exploit its potential.



References

- [1] European Commission, 'Communication From The Commission To The European Parliament, The Council, The European Economic And Social Committee And The Committee Of The Regions. The European Green Deal.', Brussels, COM/2019/640 final., 2019. Accessed: Feb. 25, 2023. [Online]. Available: <https://eur-lex.europa.eu/legal-content/EN/TXT/?uri=COM%3A2019%3A640%3AFIN>
- [2] United Nations Environment Programme, '2021 Global status report for buildings and construction: Towards a zero-emission, efficient and resilient buildings and construction sector', 2021. Accessed: Feb. 25, 2023. [Online]. Available: <https://globalabc.org/resources/publications/2021-global-status-report-buildings-and-construction>
- [3] Global Alliance for Buildings and Construction, 'Global Status Report for Buildings and Construction', 2019. [Online]. Available: <https://www.worldgbc.org/sites/default/files/2019%20Global%20Status%20Report%20for%20Buildings%20and%20Construction.pdf>
- [4] F. Krausmann *et al.*, 'Global socioeconomic material stocks rise 23-fold over the 20th century and require half of annual resource use', *Proceedings of the National Academy of Sciences*, vol. 114, no. 8, pp. 1880–1885, Feb. 2017, doi: 10.1073/pnas.1613773114.
- [5] C. Galán-Marín, C. Rivera-Gómez, and A. García-Martínez, 'Embodied energy of conventional load-bearing walls versus natural stabilized earth blocks', *Energy and Buildings*, vol. 97, pp. 146–154, Jun. 2015, doi: 10.1016/j.enbuild.2015.03.054.
- [6] R. Azari and N. Abbasabadi, 'Embodied energy of buildings: A review of data, methods, challenges, and research trends', *Energy and Buildings*, vol. 168, pp. 225–235, Jun. 2018, doi: 10.1016/j.enbuild.2018.03.003.
- [7] F. Asdrubali, G. Grazieschi, M. Roncone, F. Thiebat, and C. Carbonaro, 'Sustainability of Building Materials: Embodied Energy and Embodied Carbon of Masonry', *Energies*, vol. 16, no. 4, 2023, doi: 10.3390/en16041846.
- [8] United Nations Environment Programme and Global Alliance for Buildings and Construction, '2020 Global Status Report for Buildings and Construction: Towards a Zero-emissions, Efficient and Resilient Buildings and Construction Sector - Executive Summary', 2020, [Online]. Available: <https://wedocs.unep.org/20.500.11822/34572>
- [9] F. Kleemann, J. Lederer, H. Rechberger, and J. Fellner, 'GIS-based Analysis of Vienna's Material Stock in Buildings', *Journal of Industrial Ecology*, vol. 21, no. 2, pp. 368–380, 2017, doi: 10.1111/jiec.12446.
- [10] European Commission, 'Communication From The Commission To The European Parliament, The Council, The European Economic And Social Committee And The Committee Of The Regions. A Renovation Wave for Europe: greening our buildings, creating jobs, improving lives', 2020. Accessed: Feb. 25, 2023. [Online]. Available: <https://eur-lex.europa.eu/legal-content/EN/TXT/?qid=1603122220757&uri=CELEX:52020DC0662>
- [11] European Commission, 'Proposal for a Directive Of The European Parliament And Of The Council on the energy performance of buildings (recast)', 2021. Accessed: Feb. 25, 2023. [Online]. Available: <https://eur-lex.europa.eu/legal-content/EN/TXT/?uri=CELEX%3A52021PC0802&qid=1641802763889>
- [12] European Commission, 'Communication From The Commission To The European Parliament, The Council, The European Economic And Social Committee And The Committee Of The Regions. New European Bauhaus: Beautiful, Sustainable, Together', 2021. Accessed: Mar. 21, 2023. [Online]. Available: <https://eur-lex.europa.eu/legal-content/EN/TXT/?uri=CELEX%3A52021DC0573&qid=1679411587404>



- [13] European Commission, *Circular Economy Action Plan: the European Green Deal*. LU: Publications Office of the European Union, 2020. Accessed: Feb. 26, 2023. [Online]. Available: <https://data.europa.eu/doi/10.2775/458852>
- [14] BAMB Project Consortium, 'Buildings As Material Banks (H2020 BAMB)', *BAMB*, 2016. <https://www.bamb2020.eu/> (accessed Feb. 26, 2023).
- [15] M. Wurm, A. Droin, T. Stark, C. Geiß, W. Sulzer, and H. Taubenböck, 'Deep Learning-Based Generation of Building Stock Data from Remote Sensing for Urban Heat Demand Modeling', *IJGI*, vol. 10, no. 1, p. 23, Jan. 2021, doi: 10.3390/ijgi10010023.
- [16] H. Haberl *et al.*, 'High-Resolution Maps of Material Stocks in Buildings and Infrastructures in Austria and Germany', *Environ. Sci. Technol.*, vol. 55, no. 5, pp. 3368–3379, Mar. 2021, doi: 10.1021/acs.est.0c05642.
- [17] Y. Bao, Z. Huang, H. Wang, G. Yin, X. Zhou, and Y. Gao, 'High-resolution quantification of building stock using multi-source remote sensing imagery and deep learning', *J of Industrial Ecology*, vol. 27, no. 1, pp. 350–361, Feb. 2023, doi: 10.1111/jiec.13356.
- [18] H. Arbabi *et al.*, 'A scalable data collection, characterization, and accounting framework for urban material stocks', *J of Industrial Ecology*, vol. 26, no. 1, pp. 58–71, Feb. 2022, doi: 10.1111/jiec.13198.
- [19] D. Rajaratnam, R. A. Stewart, T. Liu, and A. S. Vieira, 'Building stock mining for a circular economy: A systematic review on application of GIS and remote sensing', *Resources, Conservation & Recycling Advances*, vol. 18, p. 200144, Oct. 2023, doi: 10.1016/j.rcradv.2023.200144.
- [20] European Commission, 'Certificates and inspections', 2023. https://energy.ec.europa.eu/topics/energy-efficiency/energy-efficient-buildings/certificates-and-inspections_en (accessed Apr. 26, 2023).
- [21] A. G. Charalambides, C. N. Maxoulis, O. Kyriacou, E. Blakeley, and L. S. Frances, 'The impact of Energy Performance Certificates on building deep energy renovation targets', *International Journal of Sustainable Energy*, vol. 38, no. 1, pp. 1–12, Jan. 2019, doi: 10.1080/14786451.2018.1448399.
- [22] Y. Li, S. Kubicki, A. Guerriero, and Y. Rezgui, 'Review of building energy performance certification schemes towards future improvement', *Renewable and Sustainable Energy Reviews*, vol. 113, p. 109244, Oct. 2019, doi: 10.1016/j.rser.2019.109244.
- [23] O. Pasichnyi, J. Wallin, F. Levihn, H. Shahrokni, and O. Kordas, 'Energy performance certificates — New opportunities for data-enabled urban energy policy instruments?', *Energy Policy*, vol. 127, pp. 486–499, Apr. 2019, doi: 10.1016/j.enpol.2018.11.051.
- [24] K. Mayer, L. Haas, T. Huang, J. Bernabé-Moreno, R. Rajagopal, and M. Fischer, 'Estimating building energy efficiency from street view imagery, aerial imagery, and land surface temperature data', *Applied Energy*, vol. 333, p. 120542, Mar. 2023, doi: 10.1016/j.apenergy.2022.120542.
- [25] Regione Lombardia, 'Database CENED+2 - Certificazione ENergetica degli EDifici | Open Data Regione Lombardia', 2023. <https://www.dati.lombardia.it/Energia/Database-CENED-2-Certificazione-ENergetica-degli-E/bbky-sde5> (accessed Apr. 27, 2023).
- [26] European Space Agency, 'Sentinel-2 - Missions - Sentinel Online', *Sentinel Online*, 2023. <https://copernicus.eu/missions/sentinel-2> (accessed Apr. 27, 2023).
- [27] OpenStreetMap Foundation, 'OpenStreetMap', *OpenStreetMap*, 2023. <https://www.openstreetmap.org/> (accessed Apr. 27, 2023).
- [28] H. Hersbach *et al.*, 'The ERA5 global reanalysis', *Q.J.R. Meteorol. Soc.*, vol. 146, no. 730, pp. 1999–2049, Jul. 2020, doi: 10.1002/qj.3803.
- [29] OpenStreetMap Foundation, 'Nominatim - OSM Geocoding API', 2023. <https://nominatim.openstreetmap.org/ui/search.html> (accessed Apr. 27, 2023).



- [30] Microsoft, 'Bing Maps API & SDK Tools | Explore Bing Maps API Platform', 2023. <https://www.microsoft.com/en-us/maps> (accessed Apr. 27, 2023).
- [31] Google, 'Google Maps Platform | Google Developers', 2023. <https://developers.google.com/maps> (accessed Apr. 27, 2023).
- [32] OpenEO, 'openEO Python Client — openEO Python Client 0.17.0a2 documentation', 2023. <https://open-eo.github.io/openeo-python-client/index.html> (accessed Apr. 27, 2023).
- [33] G. Van Rossum and F. L. Drake, *Python 3 reference manual*. Scotts Valley, CA: CreateSpace, 2009.
- [34] UN, 'UN Population Division The World's Cities in 2018; United Nations'. New York, NY, USA, 2018.
- [35] IEA, 'IEA World Energy Outlook 2020; IEA'. Paris, France, p. 214, 2020.
- [36] European Union, 'Communication from the Commission to the European Parliament, the Council, the European Economic and Social Committee and the Committee of the regions an EU strategy to harness the potential of offshore renewable energy for a climate neutral future'. in n.d.). Climate Change and Law Collection. 2020. doi: 10.1163/9789004322714_cclc_2020-0164-0816.
- [37] IEA, *IEA Renewables Information*. Overview; IEA: Paris, France, 2021.
- [38] P. Corti, P. Bonomo, F. Frontini, P. Mace, and E. B. I. P. V. S. R. Bosch, 'Building Integrated Photovoltaics: A Practical Handbook for Solar Buildings', in *Stakeholders; SUPSI–Swiss BIPV Competence Centre and Becquerel Institute*, Brussels, Belgium, 2020.
- [39] European Commission, 'Solar Energy'. 2023. [Online]. Available: https://energy.ec.europa.eu/topics/renewable-energy/solar-energy_en
- [40] J. Yu, Z. Wang, A. Majumdar, and R. Rajagopal, 'DeepSolar: A machine learning framework to efficiently construct a solar deployment database in the United States', *Joule*, vol. 2, no. 12, pp. 2605–2617, 2018, doi: 10.1016/j.joule.
- [41] J. M. Malof, R. Hou, L. M. Collins, K. Bradbury, and R. Newell, 'Automatic solar photovoltaic panel detection in satellite imagery', in *2015 International Conference on Renewable Energy Research and Applications (ICRERA)*, 2015. doi: 10.1109/icrera.2015.7418643.
- [42] G. Barbose *et al.*, 'Tracking the sun: Pricing and design trends for distributed photovoltaic systems in the United States'. 2019. doi: 10.2172/1574343.
- [43] Fraunhofer ISE, 'Recent facts about photovoltaics in Germany - fraunhofer'. 2021. [Online]. Available: <https://www.ise.fraunhofer.de/content/dam/ise/en/documents/publications/studies/recent-facts-about-photovoltaics-in-germany.pdf>
- [44] J. Hoog, S. Maetschke, P. Ilfrich, and R. R. Kolluri, 'Using satellite and aerial imagery for identification of solar PV', in *Proceedings of the Eleventh ACM International Conference on Future Energy Systems*, 2020. doi: 10.1145/3396851.3397681.
- [45] J. M. Malof, K. Bradbury, L. M. Collins, and R. G. Newell, 'Automatic detection of solar photovoltaic arrays in high resolution aerial imagery', *Applied Energy*, vol. 183, pp. 229–240, 2016, doi: 10.1016/j.apenergy.2016.08.191.
- [46] Stedin, 'Kwart van de zonnepanelen niet in Beeld'. 2018. [Online]. Available: <https://www.stedin.net/over-stedin/pers-en-media/persberichten/kwart-van-de-zonnepanelen-niet-in-beeld>
- [47] D. Stowell *et al.*, 'A harmonised, high-coverage, open dataset of solar photovoltaic installations in the UK', *Scientific Data*, vol. 7, no. 1, 2020, doi: 10.1038/s41597-020-00739-0.
- [48] M. Formolli *et al.*, 'Solar Energy in Urban Planning: Lesson learned and recommendations from six Italian case studies'. Mar. 14, 2022. [Online]. Available: <https://www.mdpi.com/2076-3417/12/6/2950>
- [49] M. M. Akrofi, '& Abstract Early integration of solar energy considerations into urban planning/design is necessary to ensure that future cities do not only consume but also produce energy locally through solar', *Yet*, Apr. 2022, [Online]. Available: <https://www.sciencedirect.com/science/article/pii/S2664328622000171>

- [50] J. M. Malof, L. M. Collins, K. Bradbury, and R. G. Newell, 'A deep convolutional neural network and a random forest classifier for solar photovoltaic array detection in aerial imagery', in *2016 IEEE International Conference on Renewable Energy Research and Applications (ICRERA)*, 2016. doi: 10.1109/icrera.2016.7884415.
- [51] L. Breiman, 'Random forests - machine learning'. 2001. [Online]. Available: <https://link.springer.com/article/10.1023/a:1010933404324>
- [52] M. (Université L. de B. (ULB)) Lennert, 'A complete toolchain for object-based image analysis with GRASS GIS', no. 163. in *FOSS4G Bonn 2016*. 2016. [Online]. Available: <https://doi.org/10.5446/20409>
- [53] T. Grippa, M. Lennert, B. Beaumont, S. Vanhuyse, N. Stephenne, and E. Wolff, 'An open-source semi-automated processing chain for Urban Object-based classification', *Remote Sensing*, vol. 9, no. 4, p. 358, 2017, doi: 10.3390/rs9040358.
- [54] A. Ng, *Machine Learning Yearning*. 2023.
- [55] Z. Rasouli and V. Puig, 'Tilt angle optimization of photovoltaic panels'. 2019. [Online]. Available: <https://www.iri.upc.edu/publications/show/2260>
- [56] B. So *et al.*, 'Estimating the electricity generation capacity of solar photovoltaic arrays using only color aerial imagery', Jul. 2017, pp. 1603–1606. doi: 10.1109/IGARSS.2017.8127279.
- [57] INE, 'Alicante/alacant: Población por municipios y sexo'. 2023. [Online]. Available: <https://www.ine.es/jaxiT3/Datos.htm?t=2856>
- [58] Ajuntamento de Crevillent, 'Agenda urbana crevillent 2030 | ayuntamiento de crevillent'. 2023. [Online]. Available: <https://www.crevillent.es/pagina/agenda-urbana-crevillent-2030/>
- [59] Global Solar Atlas, 'Photovoltaic Power Potential'. 2019. [Online]. Available: <https://globalsolaratlas.info/download/spain>
- [60] C. Enercoop, F., and Ro, 'Comunidad Energética de crevillent, así es el pionero autoconsumo colectivo que ahorra en la factura de la Luz'. Sep. 28, 2021. [Online]. Available: <https://www.grupoenercoop.es/comunidad-energetica-de-crevillent-asi-es-el-pionero-autoconsumo-colectivo-que-ahorra-en-la-factura-de-la-luz/>
- [61] IDEV, 'Ortofoto de 2022 de la Comunitat Valenciana en RGBI y de 25 cm de resolución'. 2023. [Online]. Available: https://geocataleg.gva.es/#/search?uuid=spaicv0202_2022CVL0025&lang=spa
- [62] Gobierno de España, 'Sede Electrónica del Catastro'. 2023. [Online]. Available: <https://www1.sedecatastro.gob.es/>
- [63] G. GRASS, 'i.pca'. 2023. [Online]. Available: <https://grass.osgeo.org/grass82/manuals/i.pca.html>
- [64] P. Li *et al.*, 'Understanding rooftop PV panel semantic segmentation of satellite and aerial images for better using machine learning', *Advances in Applied Energy*, vol. 4, p. 100057, 2021, doi: 10.1016/j.adapen.2021.100057.
- [65] IDEV, 'Cartografía oficial de la Comunitat Valenciana a escala 1:5.000 de l'Institut Cartogràfic Valencià'. 2023. [Online]. Available: https://geocataleg.gva.es/#/results/series_cartograficas
- [66] A. DLR, 'Orthorectification'. 2023. [Online]. Available: https://www.dlr.de/eoc/en/desktopdefault.aspx/tabid-6144/10056_read-20918/
- [67] G. GRASS, 'r.learn.ml'. 2023. [Online]. Available: <https://grass.osgeo.org/grass82/manuals/addons/r.learn.ml.html>
- [68] H. Khurshid and M. Khan, 'Segmentation and Classification Using Logistic Regression in Remote Sensing Imagery', *IEEE Journal of Selected Topics in Applied Earth Observations and Remote Sensing*, vol. 8, pp. 224–232, Jan. 2015, doi: 10.1109/JSTARS.2014.2362769.
- [69] T. Lei, S. Wan, S. Wu, and H. Wang, 'A new approach of ensemble learning technique to resolve the uncertainties of Paddy area through image classification'. Nov. 09, 2020. [Online]. Available: <https://www.mdpi.com/2072-4292/12/21/3666>



- [70] G. GRASS, 'r.neighbors'. 2023. [Online]. Available: <https://grass.osgeo.org/grass82/manuals/r.neighbors.html>
- [71] S. Ren *et al.*, 'Automated Extraction of Energy Systems Information from Remotely Sensed Data: A Review and Analysis', *Applied Energy*, vol. 326, p. 119876, 2022, doi: <https://doi.org/10.1016/j.apenergy.2022.119876>.
- [72] S. Xu, M. Sang, M. Xie, F. Xiong, T. Mendis, and X. Xiang, 'Influence of urban morphological factors on building energy consumption combined with photovoltaic potential: A case study of residential blocks in Central China', *Building Simulation*, 2023, doi: 10.1007/s12273-023-1014-4.
- [73] Mapflow, 'Mapflow AI Models'. 2023. [Online]. Available: <https://docs.mapflow.ai/>
- [74] W. Alsabhan, B. Dudin, and T. Alotaiby, 'Detecting buildings and nonbuildings from satellite images using U-Net'. 2022. [Online]. Available: <https://pubmed.ncbi.nlm.nih.gov/35571708/>
- [75] IDEV, 'Normalized Digital Surface Model (nDSM) of LIDAR of 1 meter resolution covering the province of Alicante 2016'. 2023. [Online]. Available: https://catalogo.icv.gva.es/geonetwork/srv/eng/catalog.search#/metadata/spaicv030501_2016_PALI0100
- [76] K. Poon, J. Kämpf, S. Tay, N. Wong, and T. Reindl, 'Parametric Study of urban morphology on building solar energy potential in Singapore context', *Urban Climate*, vol. 33, p. 100624, 2020, doi: 10.1016/j.uclim.2020.100624.
- [77] A. Boccalatte, M. Thebault, C. Ménézo, J. Ramousse, and M. Fossa, 'Evaluating the impact of urban morphology on rooftop solar radiation: A new city-scale approach based on Geneva GIS data', *Energy and Buildings*, vol. 260, p. 111919, 2022, doi: <https://doi.org/10.1016/j.enbuild.2022.111919>.
- [78] C. Carneiro, E. Morello, and G. Desthieux, 'Assessment of solar irradiance on the urban fabric for the production of renewable energy using LIDAR data and image processing techniques', in *Advances in GIScience*, 2009, pp. 83–112. doi: 10.1007/978-3-642-00318-9_5.



OUR TEAM



Università
Ca' Foscari
Venezia



Politecnico
di Torino



Köhler & Meinzer



TECHNISCHE
UNIVERSITÄT
WIEN
Vienna | Austria



INSOMNIA



Louvain research institute for Landscape,
Architecture, Built environment



synavision
Perfect Building Performance

See you online!



moderate-project.eu



@MODERATE_HE



MODERATE

